A Comprehensive Review on Gas Flow in Microchannels

Amit Agrawal
Department of Mechanical Engineering, Indian Institute of Technology Bombay,
Powai, Mumbai-400076, India

ABSTRACT

A review of gas flow in microchannels of different cross-sections is presented in this article. The phenomenon of slip, slip models and measurement of slip coefficient are first discussed. The planar microchannels are dealt with in great detail; the different analytical, experimental and simulation approaches and solutions available in the literature are reviewed. A review of literature on square, rectangular and circular microchannels have revealed that these microchannels have also been extensively studied. Information on other shapes of microchannels such as triangular, trapezoidal and elliptical is also presented. It is recognized that surface roughness may play an important role; therefore the effect of surface roughness on flow characteristics and overall pressure drop is given due attention. It is further recognized that frequently the microchannels may not be straight; therefore, microchannels with bends or involving sudden expansion/contraction is considered. Empirical correlations and equations are included for ready reference.

1. INTRODUCTION

Flow of gas at the microscale has fundamental differences with respect to flow at the conventional scales. The primary difference is that slipping of gas occurs at solid-gas interface, as opposed to no-slipping at the conventional scales. The flow is also usually accompanied by a substantial change in the density of the gas. These effects are generally referred to as rarefaction and compressibility effects (Beskok et al. 1996), respectively, and are measured in terms of non-dimensional parameters – Knudsen number (Kn) and Mach number (Ma). These non-dimensional parameters are related to Reynolds number (Re) as $Kn = \sqrt{\frac{\pi\gamma}{2}}\frac{Ma}{\mathrm{Re}}$ where γ is the ratio of specific heats for the gas. Interestingly, significant compressibility effects can be present at the microscale even when the Mach number is less than 0.3. The Knudsen number is a ratio of the mean free path of the gas (λ) to the characteristic length scale in the flow $\left(Kn = \frac{\lambda}{L}\right)$. The Knudsen number becomes relatively large ($Kn > 0.001$) at the microscale owing to the small length scale. The problem of gas flow therefore falls under the category of compressible internal flow with slip at the wall (Ho and Tai 1998; Sharipov and Seleznev 1998; Gad-el-Hak 1999). Recent experiments by Demsis et al. (2009, 2010a) have shown that the Nusselt number is anomalously low with gas flow, and that the available theoretical analysis are unable to correctly predict its value. Figure 1 illustrates the various flow regimes in terms of the Knudsen number and the relevant governing equations (Schaaf and Chamber 1961; Karniadakis et al. 2005; Mahulikar et al. 2007).

Knowledge of flow in microchannel is directly relevant in the design of practical devices such as micro heat exchangers (Tuckerman and Pease 1981; Khan and Fartaj 2011), micro-filter (Mott et al. 2001; Saxena et al. 2009), fuel cell (Yoon et al. 2006), etc. Study of gas flow in microchannel is also expected to influence design of numerous micro-devices such as breath analyzer, micro-nozzle and micro-thruster, safety micro-devices (where regular sampling of air is required for detection of pathogens) along with other potentially exciting applications (Ho and Tai 1998; Rostami et al. 2002;

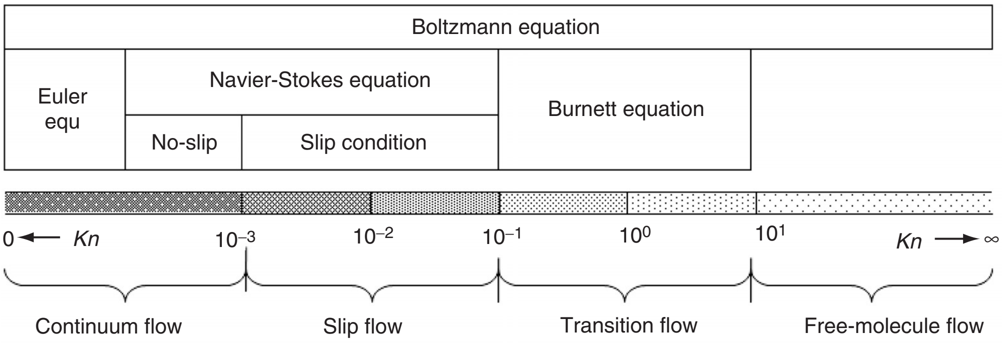

Figure 1. Flow regimes in terms of Knudsen number.

Hu and Li 2007). Understanding of gas flow and development of empirical correlations is also relevant from the standpoint of vacuum appliances and outer space applications (Reese et al. 2003).

A large number of recent studies have been undertaken on gas flow in microchannel and for rarefied gas flow in the slip and transition flow regimes in order to understand the fundamental issues, and also because of their practical relevance, mentioned above. A number of review articles are also available on the subject. Sobhan and Garimella (2001) compiled the results from early investigations on fluid flow and heat transfer in mini-channels, microchannels and microtubes. From the data compiled in Morini (2004), Hetsroni et al. (2005) and Morini et al. (2006), it is evident that several contradicting results about the value of friction factor, with respect to its value at the conventional scale, have been reported in the literature. A similar observation applies to the critical Reynolds number for transition of the flow from laminar to turbulent.

This article intends to collate information on gas flow in microchannels of different cross-sections. The emphasis however is on flow between two long parallel plates, a configuration which has received maximum attention owing to the relatively simple geometry. The problem is therefore amenable to analytical tools and the solution has been obtained through various analytical approaches. Several numerical schemes have also been developed to capture the flow behavior correctly. The numerical results are compared with experimental data and analytical solutions. In the present review article, information about different aspects of the problem has been brought together from a relatively large number of studies. In that sense the article is much more complete than the earlier reviews, although we cannot claim it to be exhaustive. Effect of surface roughness is also included, along with a brief description of flow in complex (non-straight) geometries. Some figures and key equations from the literature are included for ready reference. Similarly, empirical correlations have been collated wherever available.

The article is organized as follows: Section 1 gives a brief introduction to the problem. Section 2 discusses the phenomenon of slip and the measurement of tangential momentum accommodation coefficient. Section 3 reviews flow in plane microchannel. The section is sub-divided into theoretical, experimental and numerical investigations. Section 4 reviews flow in microduct while Section 5 reviews flow in microtube. Flow through elliptical, triangular, trapezoidal cross-sections is considered in Section 6. Section 7 presents the effect of surface roughness on the flow. Section 8 considers flow in complex microchannel. Section 9 presents conclusions and perspectives for future work.

2. PHENOMENON OF SLIP

Maxwell, based on suggestion of a reviewer, proposed the following approach to calculate the slip velocity (Kennard 1962). On a control surface, s, at a distance of $\lambda/2$, half of the molecules come from one mean free path away from the surface with tangential velocity u_λ, and half of the molecules are reflected from the surface. Maxwell assumed that a fraction σ of the molecules are reflected diffusively at the walls (i.e., their average tangential velocity corresponds to that of the wall, u_w) and the remaining $(1-\sigma)$ of the molecules are reflected specularly (i.e., without a change of their impinging velocity u_λ). Upon expanding u_λ in Taylor series and retaining terms up to second order, the following expression is obtained:

$$u_g - u_w = \frac{2-\sigma}{\sigma}\left[Kn\left(\frac{\partial u}{\partial n}\right)_s + \frac{Kn^2}{2}\left(\frac{\partial^2 u}{\partial n^2}\right)_s\right] \tag{1}$$

In the above equation, u stands for streamwise velocity, subscripts g, w and s refer to gas, wall, and control surface respectively, σ is the tangential momentum accommodation coefficient or TMAC ($\sigma = 1$ and 0 for fully diffused and specular surfaces, respectively), and n is the normal to the control surface. The TMAC is related to the tangential momentum of the incident molecules (τ_i) and the tangential momentum of reflected molecules (τ_r) as

$$\sigma = \frac{\tau_i - \tau_r}{\tau_i}. \tag{2}$$

Note that determining the value of TMAC accurately is the key to obtaining the correct slip velocity. See Kennard (1962), Wuest (1967), Knechtel and Pitts (1973), Kuscar (1974) for authoritative discussion on various aspects of accommodation coefficients.

Pan et al. (1999) suggested that TMAC depends on the temperature of wall, speed of wall, molecular mass of gas, diameter of gas molecules, number density of gas molecules, and the characteristic length scale in the flow. Similarly, it has been suggested (see Gronych et al. 2004) that the TMAC depends on the molecular mass of the gas, with a higher value for the lighter gas. One can also expect that the gas-solid pair involved, surface condition, and curvature of surface may also influence the value of TMAC (Agrawal and Prabhu 2008b). This suggests that the parameters on which the TMAC depends upon have not been fully established. Consequently, a large number of experiments for different surface-gas combinations have been undertaken; a review of the experimental values reported in the literature is provided in Section 2.2.

2.1. Slip models

Alternate models to calculate the slip velocity exists in the literature. A few of these are mentioned here. The second order slip model given by Sreekanth (1969) and used earlier by Deissler (1964) is

$$u_g - u_w = -C_1 Kn\left(\frac{\partial u}{\partial n}\right)_w - C_2 Kn^2\left(\frac{\partial^2 u}{\partial n^2}\right)_w \tag{3}$$

This is essentially of the same form as Eq. (1) with the important difference that there are two independent coefficients unlike a single coefficient ($(2-\sigma)/\sigma$) in Eq. (1). Table 1 summarizes the various values of the coefficients (C_1 and C_2) as predicted by analysis and experimental data.

Lam (see Dongari et al. 2007) suggested the following alternate form for ease of calculations:

$$u_g - u_w = \frac{2-\sigma}{\sigma}\left[\frac{Kn}{1-bKn}\left(\frac{\partial u}{\partial n}\right)_s\right] \tag{4}$$

$$b = \left[\frac{1}{2}\frac{u_o''}{u_o'}\right]_s. \tag{5}$$

As explained by Chen and Tian (2009), in the Langmuir slip model, gas molecules are assumed not to reflect directly at solid boundaries, but rather to reside on the solid surface for a brief period of time, due to the intermolecular forces between the gas molecules and the solid surface atoms. After some lag

Table 1. Values of slip coefficients proposed in the literature [from Verma et al. 2009)]. The values obtained by Sreekanth (1969), Ewart *et al.* (2007a,b) and Maurer *et al.* (2003) are experimental, whereas the remaining have been obtained from theoretical considerations.

Source	**Gas**	***Kn* range**	C_1	C_2
Sreekanth (1969)	Nitrogen	0.007–0.03	1	0
		0.03–0.13	1.1466	0
		0.13–0.237	1.1466	0.14
Ewart *et al*. (2007a)	Helium	0.009–0.309	1.052 ± 0.020	0.148 ± 0.014
	Argon	0.003–0.302	1.147 ± 0.042	0.294 ± 0.029
	Nitrogen	0.003–0.291	1.066 ± 0.088	0.231 ± 0.057
Maurer *et al*. (2003)	Helium	0.06–0.8	1.2 ± 0.05	0.23 ± 0.1
	Nitrogen	0.002–0.59	1.3 ± 0.05	0.26 ± 0.1
Ewart *et al*. (2007b)	Helium	0.03–0.7	1.26 ± 0.022	0.17 ± 0.02
Maxwell	–	–	1	0
Schamberg	–	–	1	$5\pi/12$
Chapman & Cowling	–	–	~1	~0.5
Albertoni, Cercignnani & Gotusso	–	–	1.1466	0
Deissler	–	–	1	1.6875
Cercignani	–	–	1.1466	0.9756
Hsia & Domoto	–	–	1	0.5
Mitsuya	–	–	1	2/9

in time, these molecules may reflect from the surface. This time lag causes macroscopic velocity slip given by equations (6) and (7):

$$u_s = (1-\alpha)u_g + \alpha u_w \tag{6}$$

$$\alpha = \frac{1}{1+4\omega Kn/p}. \tag{7}$$

Chen and Tian (2009) further note that the role of the coefficient ω in the above equation is similar to TMAC (or σ) in the Maxwell's model, with the important difference that its value can be determined (with a clear physical explanation) prior to simulations. A similar explanation was given by Cao et al. (2005) as the mechanism for momentum transfer between the wall and gas.

There seems to be concensus on the validity of Eq. (3). However, there is no general agreement on the values of the slip coefficients as evident from Table 1 (Dongari et al. 2007; Agrawal and Prabhu 2008b). Cercignani and Lorenzani (2010) have recently proposed a theoretical basis for the value of the slip coefficients.

Alternatively, it is believed that a Knudsen layer exists near the walls under rarefied condition and the slip boundary condition is somewhat artificial, employed to accommodate the Knudsen layer (see example, Lockerby & Reese 2008, Lockerby et al. 2004, Dongari et al. 2011 for detailed discussion). Hadjiconstantinou (2003) argues that the difference in the theoretical and experimental values of C_2 in Table 1 can be reduced on accounting for the Knudsen layer.

Some researchers instead of using the slip boundary condition preferred to use an effective viscosity to bring in rarefaction effects in the flow (Roy and Chakraborty 2007; Arlemark et al. 2010). For example, Beskok and Karniadakis (1999) suggested using a Bosanquet-type of expression given as

$$\mu_e = \mu_0 \frac{1}{1+aKn} \tag{8}$$

where a is close to 1/2 as given by Beskok and Karniadakis (1999). Michalis et al. suggested

$$\frac{1}{\mu_e} = \frac{1}{\mu_0} + \frac{1}{\mu_\infty} \tag{9}$$

where

$$\mu_0 = a_0 \rho \bar{c} \lambda \tag{10}$$

$$\mu_\infty = a_\infty \rho \bar{c} H. \tag{11}$$

which is of the same form as Eq. 8 of Beskok and Karniadakis (1999). The results from these equations have been compared against DSMC calculations.

2.2. Measurement of tangential momentum accommodation coefficient

As mentioned above, the concept of TMAC was introduced by Maxwell in order to calculate the slip velocity at the solid-gas interface. The value of TMAC is imperative in the calculation of slip velocity; importance of precise determination of TMAC therefore cannot be overstated. Although several successful studies to measure the value of TMAC have been made in the past, the investigators presented limited comparison of their measured value against those reported in the literature. This suggests that the workers are possibly unaware of other measurements. In view of this, a compilation of methods employed and the TMAC values obtained were documented by Agrawal and Prabhu (2008b). A summary of their results is presented in the following.

The popular techniques to measure the tangential momentum accommodation coefficient are the rotating cylinder method, spinning rotor gauge method, flow through microchannel, and other miscellaneous methods. The rotating cylinder method has been employed by early researchers – Timiriazeff (1913), Millikan (1923), Stacy (1923), Van Dyke (1923), Kuhlthau (1949). Agrawal and Prabhu (2008a) re-analyzed the data of Kuhlthau (1949), where dry air was used as the gas, and suggested a value of 0.74 in the Knudsen number range of 0.1 to 8.3, and 0.94 in the slip regime. Comsa et al. (1980), Gabis et al. (1996), Tekasakul et al. (1996), Bentz et al. (1997), Lord (1977), Gronych et al. (2004) employed the spinning rotor gauge method for various monatomic, polyatomic and mixture of noble gases. The value of TMAC was found to be in the range of 0.86 to 1.02. A weak dependence of TMAC on Knudsen number could be observed from the data. The measurements of Lord (1977) indicated relatively small values. The lowest values of TMAC obtained with molybdenum as the substrate was 0.20 and 0.67 for helium and argon, respectively; the value increased to 0.9 for contaminated surfaces.

Arkilic et al. (2001) performed measurements of mass flux for different pressure ratios across silicon microchannels, with argon, nitrogen, and carbon dioxide as the working fluids. Most of the TMAC values were reported to lie in the range of 0.75–0.85. Colin et al. (2004) also measured the mass flux for different pressure ratios across their microchannels made on silicon wafer, with helium and nitrogen as the gas. They found that TMAC = 0.93 fits the data best for both these gases. Hsieh et al. (2004) studied the flow of nitrogen in silicon microchannels and reported that TMAC increases from 0.3 to 0.7 over the outlet Knudsen number range of 0.001–0.01, as $Kn^{0.337}$. Jang and Wereley (2006) found a value of 0.85 for flow of air in silicon microchannels, while Cooper et al. (2004) found a value of 0.52 for flow of argon, nitrogen, and oxygen through carbon nanotubes of diameter 200 nm. Cooper et al. (2004) obtained their value by fitting the experimental data to a Navier-Stokes equation based theoretical model. Yamaguchi et al. (2011) measured TMAC of deactivated-fused silica with argon, nitrogen, and oxygen. Their results show the tangential momentum was not accommodated completely to the surface. Huang et al. (2007a) reported a value of 0.90 obtained from the pressure sensitive paint technique for measurement of pressure in microchannels. The microchannels were made of glass and air was the working fluid in their experiments.

Blankenstein (1923) reported values of 0.99, 0.99, 0.97 and 0.96 for hydrogen, helium, air and oxygen, respectively. Chiang (see Wuest 1967) used plane Couette flow for measurement of TMAC. His data suggests a value of 0.9 over the Knudsen number range of 0.05 to 5 (Agrawal and Prabhu 2008a). Suetin et al. (1973) and Porodnov et al. (1974) employed the unsteady flow method. The former authors covered a large range of Knudsen numbers ($10^{-3} - 10^{3}$) for three noble gases – helium, neon, and argon. They reported values between 0.865 to 0.975, with the values showing a weak dependence on gas and Knudsen number. The latter authors worked with six gases in the slip flow regime and found TMAC values between 0.925 and 1.010. Shields (1980, 1983) utilized the principle of measurement of sound velocity and its absorption in low pressure gas confined in a tube (made of tungsten, platinum or silver) to determine the TMAC values for helium, neon, oxygen, nitrogen, and carbon monoxide gases. They reported a substantial dependence of TMAC value on surface condition such as the substrate exposed to atmosphere or clean. Yamamoto (2002) obtained value of 0.81 and 0.19 for xenon and argon from his molecular dynamics simulation. Blanchard and Ligrani (2007) reported a dependence of value of TMAC on surface roughness with values for air on PEEK plastic varying from 0.145 to 0.885 with change in surface roughness from 770 nm to 10 nm. Chew et al. (1993) worked with seven different gases with silicon of different roughnesses and obtained values between 0.95 and 1.04 from their measurements.

The possibility of assigning a constant value for all monatomic gases over commonly available surface materials was further explored by Agrawal and Prabhu (2008b), for simplicity in applying boundary condition in theoretical analysis and numerical simulations. As evident from Fig. 2, the

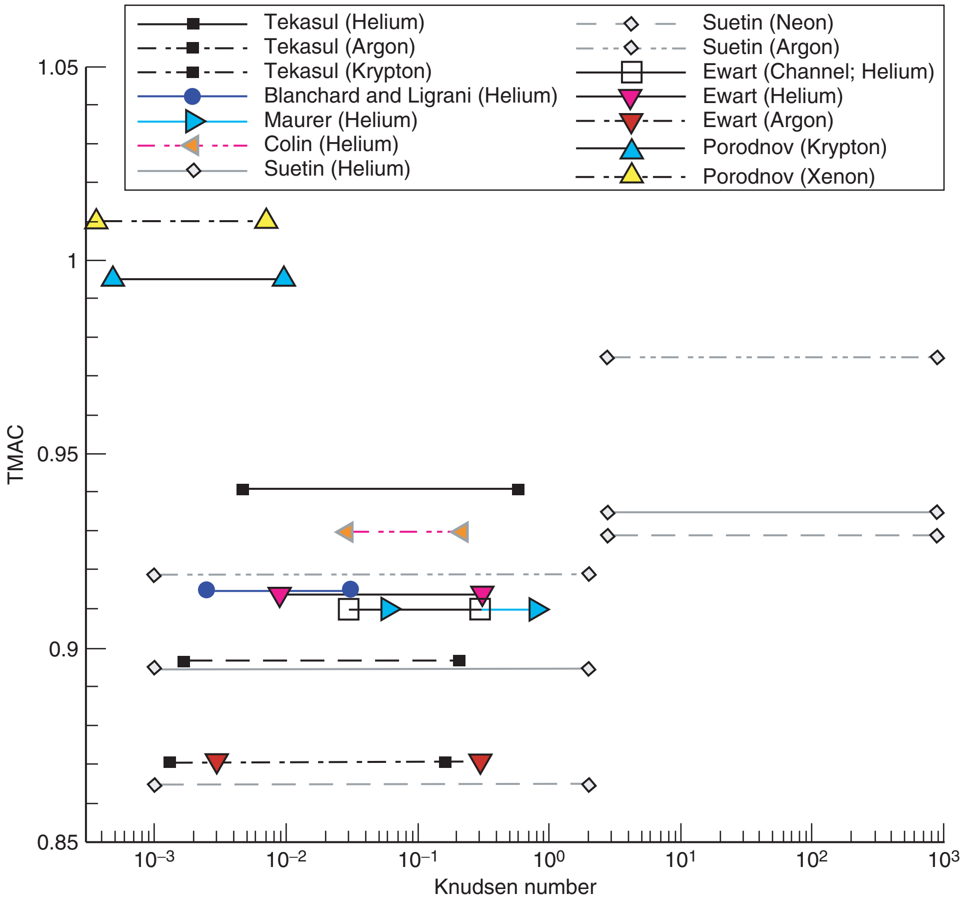

Figure 2. Variation of tangential momentum accommodation coefficient with Knudsen number for monatomic gases, as reported by different researchers. [from Agrawal and Prabhu (2008b)]

TMAC value lies in a reasonably small range, therefore employing a constant value of 0.93 for all monatomic gases over most commonly available surface materials and temperatures greater than room temperature appear reasonable (Agrawal and Prabhu 2008b). A variation in TMAC with Knudsen number for nonmonatomic gases seems to emerge from the available data (Fig. 3). In fact, Agrawal and Prabhu (2008b) suggested the following correlation for calculation of TMAC for nonmonatomic gases as a function of Knudsen number:

$$\sigma = 1 - \log(1 + Kn^{0.7}). \tag{12}$$

We would like to emphasize that data from a given technique or source should not be viewed in isolation because it may give a false impression about the trend of TMAC with Knudsen number. For example, the data of Comsa et al. (1980) suggest that TMAC for all gases is close to unity, which is not corroborated by other data in the literature. Note that data in Figs. 2 and 3 have been compiled from 14 and 16 independent measurements (with variation in either measurement technique, or gas-solid pair, or both), thereby yielding a fairly robust conclusion. Nonetheless, there is enough scope for further measurements. It is further noted that the spinning rotor gauge method and flow through microchannel have been employed by a relatively large number of researchers and yield accurate value of TMAC; these methods can therefore be employed for future measurements as well. However, further technological advancements can lead to more precise values of this important coefficient.

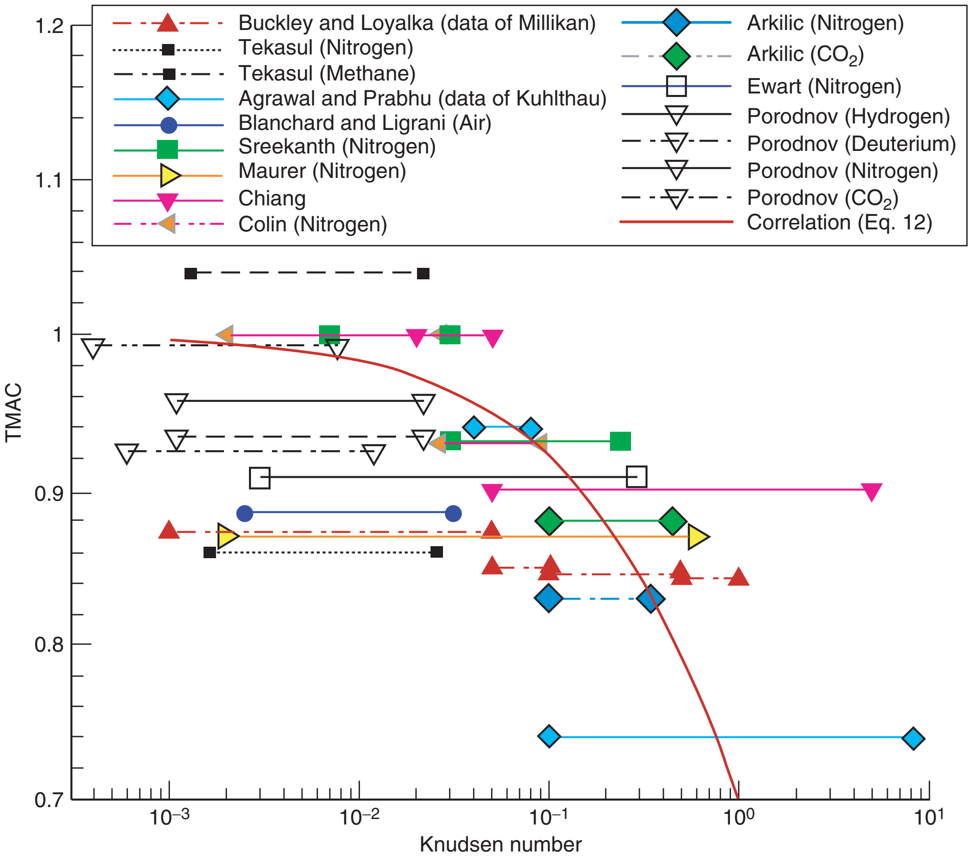

Figure 3. Variation of tangential momentum accommodation coefficient with Knudsen number for nonmonatomic gases, as reported by different researchers. The reason for the large scatter between $10^{-3} < Kn < 10^{-2}$ is discussed by Agrawal and Prabhu (2008b). [from Agrawal and Prabhu (2008b)]

3. GAS FLOW IN STRAIGHT SMOOTH MICROCHANNEL

The flow of gas between two long parallel plates separated by a small gap has been extensively studied in the past due to its fundamental significance. A large amount of experimental data, theoretical analysis performed under different sets of assumptions, and numerical solution of compressible/ incompressible governing equations with slip/ no-slip boundary condition, is therefore available.

3.1. Analytical solutions

The analytical solutions have been obtained by solving the Navier-Stokes equations, the Burnett equation or the kinetic equation. A few researchers have also proposed and solved modified forms of these equations. Similarly, different sets of boundary conditions have been utilized by different researchers.

3.1.1. Solution of Navier-Stokes equations

Harley et al. (1995) were among the first to derive analytical solution for gas flow in microchannel. They assumed flow to be compressible with no-slipping at the walls. They also solved for the case of simplified Navier-Stokes (N-S) equations with first-order slip boundary condition. Their solution suggests that the lateral velocity is non-zero in microchannel but the lateral variation in pressure and density can be neglected. Arkilic et al. (1997) solved the two-dimensional compressible Navier-Stokes equations, using perturbation analysis. The perturbation parameter chosen (ε) is the height to length ratio of the microchannel. The non-dimensional velocities and pressure after expansion in powers of (ε) were substituted into the non-dimensional governing equations, and the resulting simplified equations were such that these could be readily integrated. The lateral variation of streamwise velocity is first determined, and subsequently, the lateral velocity and streamwise variation of pressure are obtained. The resulting equations for streamwise velocity, pressure and mass flow rate are:

$$\tilde{u}_o(\tilde{x},\tilde{y}) = -\frac{\varepsilon \mathrm{Re}}{8\gamma Ma^2}\frac{d\tilde{p}_o}{d\tilde{x}}\left(1-4\tilde{y}^2+4\sigma\frac{Kn}{\tilde{p}_o}\right) \tag{13}$$

$$\tilde{p}_o(\tilde{x}) = -6\sigma Kn+\sqrt{(6\sigma Kn)^2+(1+12\sigma Kn)\tilde{x}+(P^2+12\sigma KnP)(1-\tilde{x})} \tag{14}$$

$$\dot{m} = \frac{H^3\omega P_o^2}{24\mu LRT}\left[P^2-1+12\sigma Kn(P-1)\right] \tag{15}$$

where $\tilde{u}_o$ = non dimensional streamwise velocity at inlet, $\tilde{p}_o$ = non dimensional pressure at inlet, P = inlet pressure ratio, $\dot{m}$ = mass flow rate (kg/s), H = channel height (m), ω = channel width (m), P_o = outlet pressure (Pa), μ = dynamic viscosity (Pa-s), L = length of microchannel (m), R = specific gas constant (J-kg/K), T = temperature of gas (K). Note that the obtained solution is valid for Mach and Reynolds numbers of order ε, and Knudsen number of order unity. The above conditions make the solution rather restrictive; nonetheless these equations have been widely adopted in the microfludics community for validating their experimental or numerical data.

Zohar et al. (2002) also solved the compressible Navier-Stokes equations for Knudsen number on the order of 0.1, with first-order slip boundary conditions. The Navier-Stokes equations were transformed to a second-order non-linear ordinary differential equation by suitable change of variables. The resulting equation was solved using the perturbation technique. The resulting pressure distribution agreed within 0.5% with the solution of Arkilic et al. (1997). Zhang et al. (2008) solved the incompressible form of simplified N-S equations using homotopy analysis method. They derived solutions for both the first-order and second-order slip boundary conditions. The authors noted that the obtained results using their approach are almost the same as that obtained earlier by Dongari et al. (2007). Rashidi et al. (2011) solved the incompressible form of simplified N-S equations along with the first-order slip boundary condition. The equations were solved using variational iteration method up to first-order. Djordjević (2008) proposed a new slip model and used it to derive analytical solution with simplified momentum equations. Dongari et al. (2007), Zhang et al. (2008), Rashidi et al. (2011) and Agrawal and Dongari (2011) have noted that first-order slip boundary condition (i.e., $C_2 = 0$ in Eq. 3) is not suitable for high Knudsen number flow, rather the boundary condition needs to be augmented to second-order slip condition.

Shen (2005) suggested use of degenerated Reynolds equation for solving the microchannel flow problem. The obtained results were compared against DSMC calculations.

The above approaches are for solving the differential form of the momentum equations, whereas Dongari et al. (2007) solved the integral form of the momentum equations. In their approach, the solution was obtained with the non-linear terms retained in conjunction with second-order slip boundary conditions. The solution proceeds by substituting the velocity profile, satisfying the slip boundary condition, in the governing equation, and integrating the resulting equation, which yields equation 16:

$$\begin{aligned}&\left(\frac{p}{p_0}\right)^2 - 1 + 24C_1Kn_0\left(\frac{p}{p_0}-1\right) + 96C_2Kn_0^2\log\left(\frac{p}{p_0}\right)\\&+ 2\,\mathrm{Re}^2\beta\chi\left\{12C_1Kn_0\left(\frac{p_0}{p}-1\right)+24C_2Kn_0^2\left[\left(\frac{p_0}{p}\right)^2-1\right]-\log\left(\frac{p}{p_0}\right)\right\} = -96\,\mathrm{Re}\,\beta\frac{z-z_0}{D_h}\end{aligned} \tag{16}$$

where, $\beta = \dfrac{\mu^2RT}{p_0^2D_h^2}$

$$\chi = \frac{1}{A}\int\left(\frac{u}{\bar{u}}\right)^2 dA = \left[\frac{\frac{1}{30}+\frac{2}{3}C_1Kn+\frac{8}{3}C_2Kn^2+4C_1^2Kn^2+32C_1C_2Kn^3+64C_2^2Kn^4}{\left(\frac{1}{6}+2C_1Kn+8C_2Kn^2\right)^2}\right] \tag{17}$$

$$u(y,z) = \frac{\mathrm{Re}\,\mu RT}{p(z)D_h}\left(\frac{y/H-(y/H)^2+2C_1Kn(z)+8C_2Kn^2(z)}{\frac{1}{6}+2C_1Kn(z)+8C_2Kn^2(z)}\right) \tag{18}$$

Subsequently, the cross-stream velocity (Eq. 19) and mass flow rate (Eq. 20) can be obtained from continuity equation and integrating the mass across the cross-section of the microchannel:

$$\begin{aligned}v(y,z) = {}&\frac{12C_1Kn(z)+96C_2Kn^2(z)}{1+12C_1Kn(z)+48C_2Kn^2(z)}\left(\frac{\mathrm{Re}\,\mu RT}{D_h}\right)\frac{1}{p^2(z)}\frac{dp}{dz}\\&\left\{y\left(1-\frac{3\frac{y}{H}-2\left(\frac{y}{H}\right)^2+12C_1Kn(z)+48C_2(Kn(z))^2}{1+12C_1Kn(z)+48C_2(Kn(z))^2}\right)\right\}\end{aligned} \tag{19}$$

$$\dot{m} = \left[\frac{-a_2+\sqrt{a_2^2-4a_1a_3}}{2a_1}\right]\frac{\mu}{2} \tag{20}$$

$$a_1 = 2\beta\chi\left[12C_1Kn_0(\gamma - 1 + 24C_2Kn_0^2(\gamma^2 - 1) + \log\gamma\right]$$

$$a_2 = 48\beta L/H$$

$$a_3 = \left(\frac{1}{\gamma^2} - 1\right) + 24C_1Kn_0\left(\frac{1}{\gamma} - 1\right) - 96C_2Kn_0^2\log(\gamma)$$

In the above equations: p = pressure (Pa), p_0 = pressure at reference position z_0 (Pa), C_1, C_2 = first and second order slip coefficients (see Eq. 3), Kn_0 = Knudsen number at reference point z_0, D_h = hydraulic diameter of channel (= twice the distance between the plates), z = streamwise coordinate (m), u = longitudinal velocity (m/s), v = lateral velocity (m/s). Note that the solution is in terms of both Knudsen and Reynolds numbers, and different values of slip coefficients can be evaluated from the solution. Dongari et al. (2007) further showed that their solution (but with modified values of slip coefficients) compares favorably with that of the analysis of Cercignani and Daneri (1963), Cercignani et al. (2004) and the experimental data of Dong (see Cercignani and Daneri 1963) up to Knudsen number as high as five. Further, the solution reduces to that obtained by Arkilic et al. (1997) under the set of assumptions employed by Arkilic et al. (1997). The solution of Dongari et al. (2007) therefore appears to be the most general solution of gas flow in a long microchannel.

Li, Xia and Du (see Guo and Li 2003) assumed that the velocity can be divided into two parts: a parabolic component and another component resulting from flow compressibility. Solution of the momentum equations yields the following correlations for streamwise velocity and friction factor:

$$u^* = \frac{Ma^{2/(n+1)}}{Ma_0^{2/(n+1)}}\left[2(1 - r^{*^2}) + \frac{2}{n+1}\frac{Ma_{x^*}}{Ma}\left(\frac{r^{*^2}}{2} - \frac{r^{*^4}}{2} + \frac{r^{*^6}}{9} - \frac{1}{9}\right)\right] \tag{21}$$

$$f = \frac{64}{\text{Re}} + \frac{64}{\text{Re}}\frac{Ma^2}{1.5 - 0.66Ma - 1.14Ma^2} \tag{22}$$

Note the dependence of friction factor on Mach number. Vimmr et al. (2010) solved the Oseen's equation along with first-order slip model. They obtained the following expression for velocity.

$$\tilde{u}(\tilde{x},\tilde{y}) = \tilde{u}_o(\tilde{x},\tilde{y}) + 2\sum_{k=1}^{\infty}\frac{\Phi(\mu_k,\tilde{y})}{\Psi'(\mu_k)}e^{-\frac{\mu_k^2}{\text{Re}\,\tilde{h}^2}\tilde{x}} \tag{23}$$

where

$$\tilde{u}_o(\tilde{x},\tilde{y}) = 2\lim_{\mu_0\to 0}\frac{\Phi(\mu_0,\tilde{y})}{\Psi'(\mu_0)}e^{-\frac{\mu_0^2}{\text{Re}\,\tilde{h}^2}\tilde{x}} = \frac{1 + 2\frac{Kn}{\tilde{h}} - \frac{\tilde{y}^2}{\tilde{h}^2}}{\frac{2}{3} + 2\frac{Kn}{\tilde{h}}} \tag{24}$$

$$\Phi(\mu_k,\tilde{y}) = \cos\left(\frac{\mu_k}{\tilde{h}}\tilde{y}\right) - \cos\mu_k + Kn\frac{\mu_k}{\tilde{h}}\sin\mu_k \tag{25}$$

$$\Psi'(\mu_k) = \left[\mu_k\left(1 + \frac{Kn}{\tilde{h}}\right) - \frac{1}{\mu_k}\right]\sin\mu_k + \left(1 + \frac{Kn}{\tilde{h}}\mu_k^2\right)\cos\mu_k \tag{26}$$

and $\mu_{k,}$ $k = 1, 2\ldots$ are roots of the transcendent equation

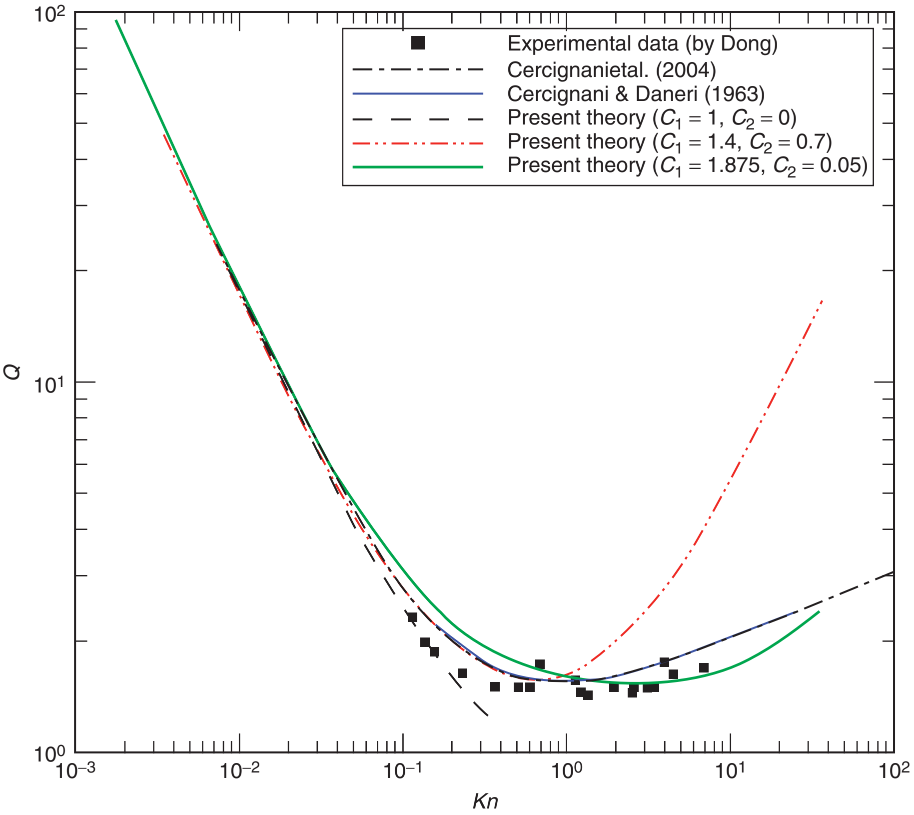

Figure 4. Comparison of normalized volume flux versus Knudsen number, against the theoretical results obtained by Cercignani et al. (1963, 2004). [from Dongari et al. (2007)]

$$\cot \mu = \frac{1}{\mu} + \frac{Kn}{\tilde{h}} \mu \tag{27}$$

Dongari et al. (2009a, 2009b) solved the "extended" Navier-Stokes equations along with the no-slip boundary condition. The extended equations have been proposed by Durst et al. (2006) and include an additional mass flux term, induced due to the self-diffusion of mass; see also Brenner (2005). Due to this term the continuity equation, stress terms and heat flux terms get modified. Dongari et al. (2009a, 2009b) showed that the solution of the extended equations agrees with the experimental data of Maurer et al. (2003). They further showed that this additional mass flux term can become of comparable order to the mass flux in microchannel. Interestingly, this approach could resolve the Knudsen minima. Dongari et al. (2010a) solved the modified Navier-Stokes equations with appropriate Fick's diffusive flux terms added to continuity and momentum equations. Dongari et al. (2010b) solved the modified N-S equations suggested by Chakraborty and Durst (2007) and validated the resulting solution against DSMC calculations.

3.1.2. Solution of Burnett and kinetic equations

The Navier–Stokes equations are not appropriate to model the gas flow in the transition regime (see Fig. 1); however, the higher-order Burnett equations can be used in this regime (Agarwal et al. 2001). The Burnett equations are derived from the Boltzmann equation using the Chapman–Enskog expansion with Knudsen number as a parameter (Chapman and Cowling, 1970).

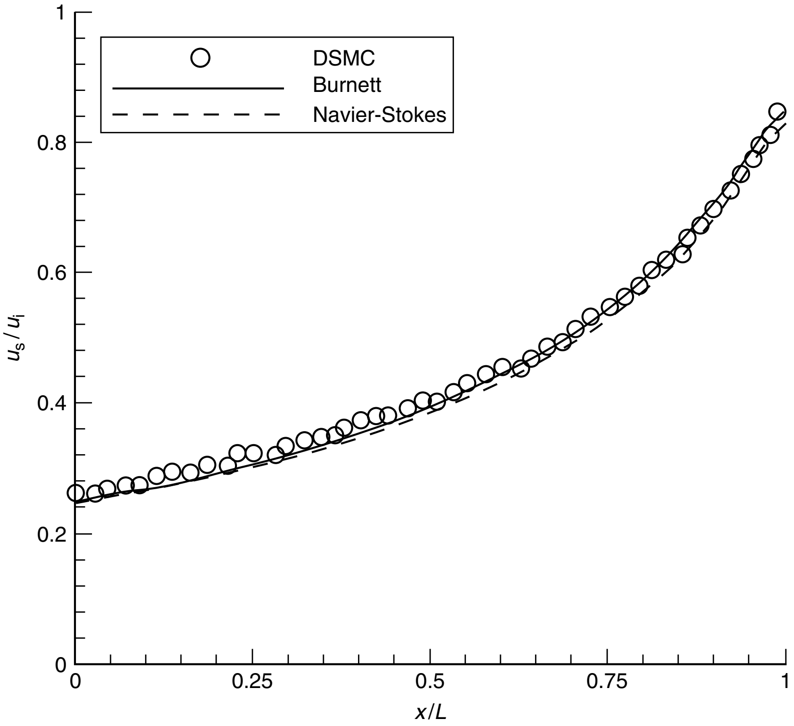

Figure 5. Slip velocities along the channel wall. [from Bao and Lin (2008)]

Bao and Lin (2008, 2009) solved the Burnett equations with slip boundary condition. Their results were found to compare well with the DSMC computations of Beskok (2001). For example, Fig. 5 shows the slip velocities along the channel wall, which agree well with those from DSMC calculations. In summary, convergent solutions were obtained up to $Kn = 0.4$. Whereas in the slip flow regime the Burnett equations and N-S equations gave almost the same result, in the transition regime the Burnett equations show better agreement with experimental and DSMC results.

Xu (2003) and Xu and Li (2004) examined the cross-stream variation of pressure at $Kn = 0.1$ and Reynolds number of order one. They argued that for the pressure driven case, the Navier–Stokes and the DSMC results exhibit opposite trends for pressure distribution in the cross-stream direction. However, the result calculated by the BGK-Burnett scheme is consistent with the DSMC solution, which suggests that the non-constant pressure in the Poiseuille flow comes from the Burnett order.

Aoki et al. (2002) performed a systematic asymptotic analysis for small Knudsen numbers as well as a direct numerical analysis on the basis of kinetic theory for flow of a rarefied gas between two parallel plates. Zahmatkesh et al. (2011) extended the velocity-slip and temperature-jump boundary conditions to simulation of flow of gas mixture in microgeometries. They solved the ensuing equations for helium-neon mixture. Other studies involving solution of kinetic equations are by Cercignani and Daneri (1963), Cercignani et al. (2004), among others.

3.2. Experimental studies in microchannel

Measurements of pressure as a function of streamwise position and mass flow rate as a function of pressure ratio across the microchannel have been reported in the literature. Measurement of velocity is much more challenging and its measurement is limited to that by Sreekanth (1969), who used a scaled-up experimental facility. Some effort to perform measurements with gas at microscale (channel size of 1–2 mm) has however been made by Yoon et al. (2006). Morini et al. (2011) have recently reviewed the experimental techniques that have been employed for measurements of flow in microchannel.

Pfahler et al. (1991), Choi et al. (1991), Pong et al. (1994), Liu et al. (1995), Harley et al. (1995), Shih et al. (1996) were some of the early researchers who made measurements in microchannels. Pong et al. (1994) measured pressure in rectangular microchannels (5–40 micron wide, 1.2 micron deep and 3 mm in length) as a function of streamwise position with nitrogen and helium as the working gas. Their data has subsequently been widely used for validation of theoretical and numerical results. Harley et al. (1995) performed measurements in 1 cm long, 100 micron wide, and 0.5–20 micron deep microchannels of either rectangular or trapezoidal cross-section. Nitrogen, helium, and argon were used as the gases in their experiments. The measured friction factor was compared to the theory derived by them and found to be in good agreement with the theoretical predictions.

Hsieh et al. (2004) worked with microchannel microfabricated on an oxidized silicon wafer and nitrogen gas. The microchannel was 50 micron deep, 200 micron wide and 24 mm long. The range of Knudsen and Reynolds numbers was 0.001–0.02 and 2.6–89.4, respectively. They measured the inlet and outlet pressure and use the analytical solution of Arkilic et al. (2001) to obtain pressure at intermediate positions in the microchannel.

Huang et al. (2007a) used a molecular sensor (pressure sensitive paint) to measure the pressure inside the microchannel. The dimensions of their microchannel are: 76 micron height, 6 mm width, and 25 mm length. They worked with air in the Knudsen number range of 0.003–0.4 and could achieve a spatial resolution of 5 microns with this technique. They noted that these molecular sensors are particularly sensitive below pressures of 1 psi (6895 Pa) and can also be used in complex microchannels (such as with a sharp tip or corner). Their measurements agreed reasonably well with the analytical solution of Arkilic et al. (1997). The technique was also applied to study the pressure variation in the entrance region of microchannel.

Vijayalakshmi et al. (2009) measured the pressure distribution in the microchannel. They employed trapezoidal cross-section microchannel with 61–211 micron hydraulic diameter and length of 52 mm. The authors noted differences between the experimental values and classical correlations, owing to compressible flow and turbulent effects at the microscales. Pitakarnnop et al. (2010) performed measurements over a wide range of parameters and compared their data with solution of kinetic equations. Kohl et al. (2005) performed experiments with both air and water. They did not find evidence of early transition to turbulence at the microscales. They further suggested that the friction factor can be obtained from conventional correlations.

3.3. Numerical simulation of flow in microchannel

Different techniques involving solution of N-S equations and particle based methods have been employed in the literature. Results from these techniques are briefly discussed below.

3.3.1. Numerical solution of Navier-Stokes equations

Hong et al. (2007) solved the compressible form of N-S equations along with first-order slip boundary condition (together with temperature equation) using the arbitrary-Lagrangian-Eulerian method. They simulated microchannels with height of 2, 5 and 10 microns with a fixed length to height ratio (= 200). The inlet flow is uniform while a parabolic velocity profile is obtained at the exit. They suggested the following correlations for constant wall temperature condition from their computations. For the no-slip case, they obtained

$$f_f \mathrm{Re} = 96 + 5.02Ma + 13.12Ma^2 + 76.69Ma^3 \tag{28}$$

$$f_d \mathrm{Re} = 96 + 15.03Ma + 59.28Ma^2 + 414.31Ma^3 \tag{29}$$

where f_f and f_d are Fanning and Darcy friction factors, respectively. For slip at the wall, they obtained:

$$f_f \mathrm{Re} = \frac{96}{1+12Kn} + \frac{5.02Ma + 13.12Ma^2 + 76.69Ma^3}{(1+12Kn)^2} \tag{30}$$

$$f_d \,\mathrm{Re} = \frac{96}{1+12Kn} + \frac{15.03Ma + 59.28Ma^2 + 414.31Ma^3}{(1+12Kn)^2} \tag{31}$$

f_fRe and f_dRe values obtained by this equation lies within the accuracy of 2% with the experimental data for Mach number of range of $0.2 < Ma < 0.3$.

Roy et al. (2003) solved the compressible N-S equations, using the finite element method. They employed the first-order slip boundary condition and assumed complete accommodation at the walls. The simulations were validated by comparing against the experimental data of Pong et al. (1994). Palle and Aliabadi (2011) proposed a hybrid finite element/finite volume method for simulation of flow at the microscale. Raisee and Vahedi (2010) performed simulations and numerically evaluated different slip models. Lewandowski et al. (2009) performed simulations for $Kn < 0.01$ and $\mathrm{Re} < 500$ and focused on the entrance region.

3.3.2. DSMC computations

The DSMC method was introduced by Bird in the early 1960s (see Bird 1994). Piekos and Breuer (1996), Mavriplis et al. (1997) and Oh et al. (1997) were among the first to employ this method for simulation of gas flow in microchannel. Fang and Liou (2002) simulated the micro-Couette and micro-Poiseuille flow in the Knudsen number range of 0.06 and 0.72 and compared their solution against analytical results. They noted that the solution agrees better with the higher-order boundary condition solution as compared to first-order, especially at high Knudsen numbers. The good comparison with analytical solution was seen as validation of the method in simulating such problems (Xue et al. 2000). Sun and Faghri (2000) performed DSMC calculations to study the effect of rarefaction and compressibility on the flow with nitrogen as the working gas. Knudsen number in the range of 0.03 to 0.11 was employed in the calculations. It was concluded that compressibility makes the axial pressure variation nonlinear and enhances the local friction coefficient. Yan and Farouk (2002) carried out fluid flow and heat transfer computations with different gases – nitrogen, argon, hydrogen, oxygen and noble gas mixtures. Hsieh et al. (2010) performed computations with nitrogen and suggested that DSMC should be employed for flows with Knudsen number greater than 0.01.

Fan and Shen (2001), Shen et al. (2003) and Cai et al. (2000) solved for low speed flows in long micro-channel (along with other flows) using DSMC and compared their solution with the available experimental results. These researchers employed the information preservation method (proposed by Fan and Shen) for reduction in the computational time. The information preservation method was later employed by Sun and Boyd (2002) for computation of thermal Couette flow problem at relative large Knudsen numbers. Chun and Koch (2005) also considered the issue of the random thermal motion of the gas dominating over the bulk flow velocity leading to statistical error in the computations. They proposed a numerical scheme to overcome this problem and tested it for flow in microchannel for a large range of Knudsen number.

Wang and Li (2003) performed fluid flow and heat transfer simulations at small scales for a binary gas (nitrogen). Wang and Li (2004a) and Wu et al. (2001) focused on the issue of implementation of boundary condition in DSMC. The former authors tested their method for flow in a microchannel. Wang and Li (2004) examined the application of DSMC to simulation of dense gases. As noted by Alexander et al. (1995), the collision rate for dense gas gets enhanced due to the volume occupied by the gas molecules, which alters the transport properties of the gas. This makes DSMC inconsistent for dense gases. Yang et al. (2010) suggested improvement in implementation of pressure boundary condition. This is important because flow in experiments is usually pressure driven; the values of pressure at inlet and outlet of the microchannel are therefore known and needs to be inputted in the simulations for direct comparison. Nedea et al. (2005) proposed a scheme to couple DSMC with the molecular dynamics technique.

3.3.3. Lattice Boltzmann method

The Lattice Boltzmann Method (LBM) based computation of gas flow at the microscales is an attractive alternative as compared to Molecular Dynamics and DSMC due to the high computational cost of the latter techniques. Similarly, solution of the Boltzmann equation is complicated because it requires integration of a six-independent-variables function (Shu et al. 2005). Since LBM solves a simple collision term (Bhatnagar et al. 1954; Benzi et al. 1993; Succi 2001; Li and Kwok 2003) and the number of particles in the computational domain is not related to the total number of particles, LBM is computationally more efficient than MD and DSMC (Shu et al. 2005).

Nie et al. (2002) and Lim et al. (2002) almost at the same time suggested modifications to the standard Lattice Boltzmann Method (LBM) in order to simulate flow at the microscales. According to Nie et al. (2002), the modified relaxation time (τ') is related to the standard relaxation time (τ), flow density (ρ) and reference density (ρ_0) as:

$$\tau' = \frac{1}{2} + \frac{\rho_0}{\rho}\left(\tau - \frac{1}{2}\right) \tag{32}$$

Lim et al. (2002) suggested

$$\tau = Kn\left(N_y - 1\right) \tag{33}$$

where N_y is the number of mesh points in the lateral direction. These and other (Zhang et al. 2005a; Lee and Lin 2005; Agrawal and Agrawal 2006; Zhou et al. 2006; Shirani and Jafari 2007; Ahmed and Hecht 2009; Sidik et al. 2010) researchers have shown that LBM gives good results in the slip flow regime. Subsequently, Ansumali and Karlin (2002), Niu et al. (2004, 2005), Tang et al. (2005), Tian et al. (2007), Huang et al. (2007b) have proposed several modifications to the standard scheme of LBM. These schemes are geared towards handling the relaxation time or boundary condition in a more appropriate manner. For example, Succi (2002) and Zhang et al. (2005b) added a specular reflection term to the bounceback scheme. Guo et al. (2007) considered a combination of bounce-back and specular-reflection schemes.

However, Shen et al. (2004) cautioned about employing LBM for high Knudsen number flows ($Kn > 0.194$). Guo et al. (2006) argued that because the mean free path of confined gas reduces, the relaxation time also changes. They suggested a simplified fit to Stops's function (Stops 1970) to compute the modified relaxation time.

$$\tau' = \tau \frac{2}{\pi} \tan^{-1}\left(\frac{\sqrt{2}}{Kn^{3/4}}\right) \tag{34}$$

The results from the original (Nie et al. 2002) and modified relaxation time scheme were still found to deviate from the DSMC solution at high Knudsen numbers (> 0.194) – although the modified equations performed somewhat better. Verhaeghe et al. (2009) suggested using multiple-relaxation times scheme. They showed that the proposed scheme could capture the flow behavior correctly at $Kn = 0.194$, although differences were noted when Knudsen number is increased further to 0.388. They suggested employing either higher-order velocity derivatives or a more sophisticated model (such as Cercignani-Lampis model (Cercignani and Lampis, 1971) having more than one accommodation coefficient in order to extend the validity of LBM to the transition regime.

Guo et al. (2008) proposed a generalized lattice Boltzmann equation with effective relaxation times based on a recently developed generalized Navier-Stokes constitution of Guo et al. (2007) for nonequilibrium flows. They considered the flow in the transition regime and showed that they could also capture the Knudsen minima from their simulations reasonably accurately (Fig. 6). Liu and Guo (2011) considered flow in the transition regime and showed that their simulations result compare well with that obtained by DSMC even at a Knudsen number of 0.388. They could also capture the Knudsen minima from there simulations. They further suggested that use of multiple relaxation time LBE model may overcome the problem at large Knudsen numbers.

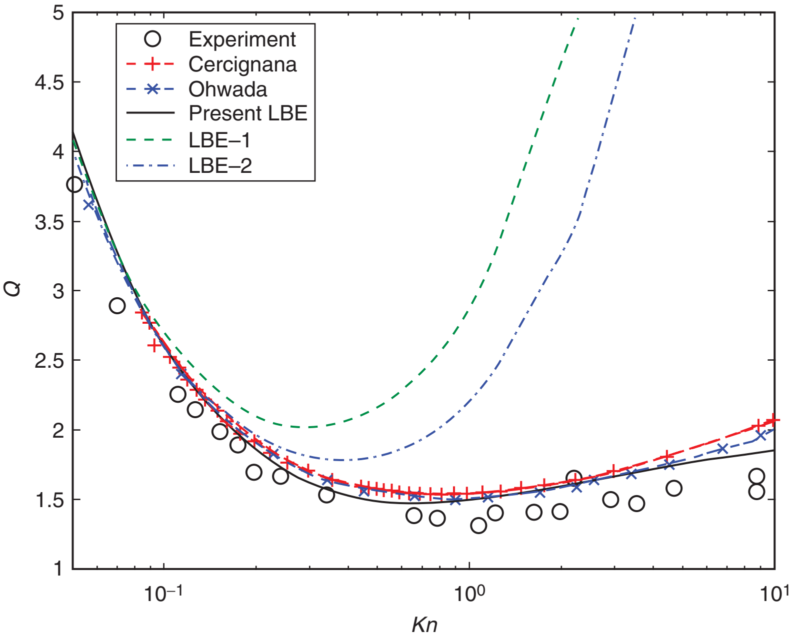

Figure 6. Mass flux of the Poiseuille flow against the Knudsen number. [from Guo et al. (2008b)]

Ansumali et al. (2006) proposed the Entropic Lattice Boltzmann Method because it is unconditionally stable for flows at low Mach numbers. Further, it is much more compliant with the boundary conditions. Li et al. (2011) implemented the Bosanquet-type effective viscosity model of Michalis et al. (2010) (Eq. 9 above). Toschi and Succi (2005) added a virtual wall collision term in the probability distribution of the particles. Chen and Tian (2009) suggested using the Langmuir slip model (instead of the standard Maxwell's model) for simulation of the flow. They tested this model on two flows –micro-Couette flow and isothermal micro-Poiseuille flow. Harting et al. (2010) recently reviewed the slip models that have been proposed and implemented with LBM. Sofonea and Sekerka (2005) discretized the Boltzmann equation using the finite difference method. The resulting equations are therefore different than the standard LBM equations.

There is still challenge in using LBM for flow in the transition regime. This is because the third order and higher order spatial derivatives involved in the Burnett or super-Burnett equations, are not captured by the lattice Boltzmann equation (Guo et al. 2006). The scheme of Guo et al. (2008) however shows promise in simulating high Knudsen number flows; these should be tested in other geometries and flow conditions for its robustness.

4. FLOW IN A MICRO-DUCT

Frequently, the width to height ratio (aspect ratio) of a microchannel is finite implying that the effect of the lateral walls on the flow should be taken into account. The aspect ratio therefore becomes another independent parameter for flow in a micro-duct. While the cross-section of micro-duct is rectangular in general, a square cross-section is recovered for unity aspect ratio. The flow is three-dimensional in nature (with all three velocity components being non-zero in general) and therefore more difficult to solve analytically than the two-dimensional flow in a microchannel. Numerical simulation of the flow is also computationally more expensive.

Jang and Wereley (2004) obtained an analytical solution for slip flow in a microduct. They obtained the following expression for streamwise variation of pressure:

$$\frac{P}{P_o}=-\frac{CP2}{CP1}Kn_o+\left\{\left(\frac{CP2}{CP1}Kn_o+\frac{P_i}{P_o}\right)^2-\left[\left(\frac{Pi}{P_o}\right)^2-1+2\frac{CP2}{CP1}Kn_o\left[\frac{P_i}{P_o}-1\right]\right]\frac{x}{L}\right\}^{1/2} \tag{35}$$

where CP1 and CP2 depend on the aspect ratio (the expressions for CP1 and CP2 are given in Jang and Wereley 2004). Agrawal and Agrawal (2005) were the first to simulate flow in square and finite aspect ratio rectangular cross-section microchannels and obtain detailed information about the flow. They used LBM for simulating the flow. Agrawal and Agrawal (2006) reported that the pressure in square microduct behaves somewhat similar to two-dimensional microchannels. The pressure distribution was found to be in good agreement with the analytical solution of Jang and Wereley (2004). Interestingly, they found that the slip velocity at the impenetrable wall has two components: along and perpendicular to the primary flow direction. A detailed analysis of the velocity behavior suggested that the velocity component along the depth is never identically zero, implying that the flow is not truly two-dimensional, although for practical purposes a two-dimensional treatment might suffice.

Renksizbulut et al. (2006) solved the three-dimensional incompressible form of N-S equation (along with the energy equation) and first-order velocity slip (and temperature jump) boundary condition. They noted that the Fanning friction factor times Reynolds number at the entrance is finite with a value of $2(2-\sigma)/(\sigma \cdot Kn)$; they further noted that this value is independent of the geometry because this relationship applies at a location where fluid is about to enter the microchannel, where there is no recognition of the geometry.

Hettiarachchi et al. (2008) employed the finite volume method to solve the three-dimensional incompressible form of N-S equation along with the energy equation. Because of inherent symmetry in the geometry, only a quarter of the channel is considered in the analysis. Their code gave the correct value of f.Re for the no-slip case as confirmed by comparing against the correlation of Shah and London (1978). For the case with slip, they proposed the following correlation:

$$f\,\mathrm{Re}_{Kn} = \frac{1}{1+(11.93-11.32/\alpha+10.32/\alpha^2-3.15/\alpha^3)Kn}\,f\,\mathrm{Re}_{Kn=0} \tag{36}$$

The variation of entrance length on the Knudsen number and microchannel aspect ratio was also presented in this work (Fig. 7).

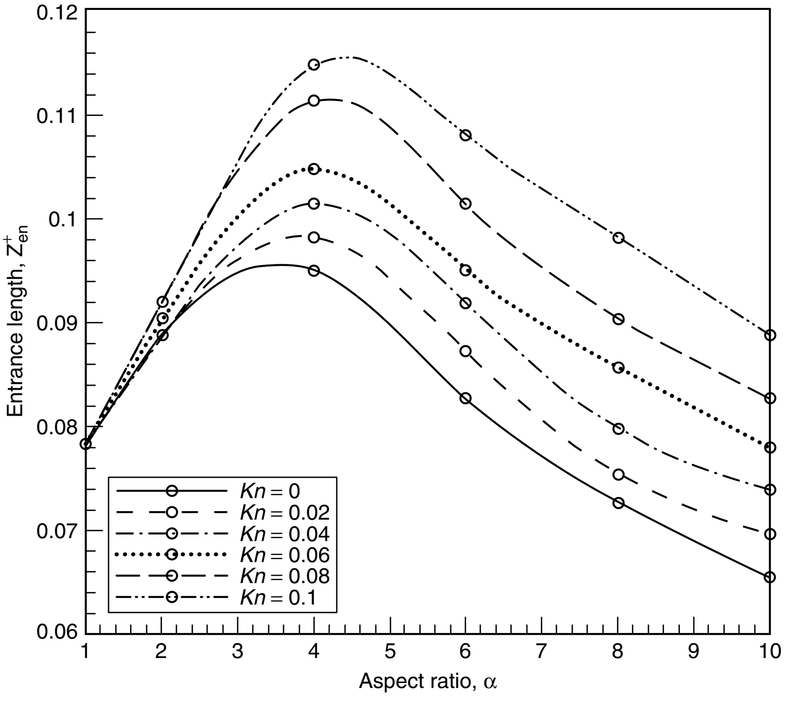

Figure 7. Variation of entrance length with channel aspect ratio at different Knudsen number (*Kn*) values. [from Hettiarachchi et al. (2008)]

Zhang et al. (2009) solved the three-dimensional compressible form of N-S equation along with first-order slip boundary condition, using a commercial code. They assumed that the fluid viscosity is a function of Knudsen number and varies as

$$\mu_{eff} = \frac{\mu}{1 + 9.638 Kn^{1.159}} \tag{37}$$

They also studied the effect of TMAC on the solution. They proposed the following correlation in terms of slip length (L_s):

$$f\,\mathrm{Re} = 56.43 e^{-2.427 L_s / D_h} \tag{38}$$

Verma et al. (2010) performed measurements for flow in a smooth square tube. They proposed the following correlation which is valid in the range $0.0022 < Kn < 0.024$ and $0.54 < \mathrm{Re} < 13.2$ range:

$$f\,\mathrm{Re} = \frac{57}{1 + 34.5 Kn} \tag{39}$$

The authors further showed that the above equation fits their data much better as compared to the correlation suggested by Morini et al. (2004a).

5. FLOW IN A MICROTUBE

Flow in a circular cross-section tube is another simple geometry, which has been extensively studied. Early researchers (Knudsen 1950, Wu and Little 1983) have either worked with fine capillaries or worked with conventional tube under reduced pressure (Brown et al. 1946, Sreekanth 1969).

Knudsen was among the first investigators to make measurements in small capillaries (see Knudsen 1950; Saha and Srivastava 1958). He worked with carbon dioxide as the gas at an average temperature of 25°C flowing in a capillary of radius 33.3 micron and length of 2 cm. Brown et al. (1946) studied flow of air through copper pipes of radius 0.795, 1.3 cm and iron pipes of radius 2.64, 5.12 and 10.1 cm under low pressure condition. They also studied flow of hydrogen in a copper pipe of radius 1.3 cm. A correlation was proposed for conductance (volume flow rate per unit pressure drop), which fits the data well for flow through copper tubes and glass capillaries. Sreekanth (1969) obtained the analytical solution for flow of rarefied gas in a tube. The solution was obtained by assuming a parabolic velocity profile, satisfying second-order slip boundary condition. This velocity profile was substituted into the integral form of the momentum equation, which was subsequently integrated. As per the analytical solution, the streamwise variation of pressure is given by

$$\begin{aligned}&\left(\frac{p}{p_0}\right)^2 - 1 + 16 C_1 Kn_0 \left(\frac{p}{p_0} - 1\right) + \frac{8}{3}\mathrm{Re}^2 \beta \left[\frac{2C_1 Kn_0 \left(p/p_0 + 24 C_1 Kn_0\right)}{\left(p/p_0 + 8C_1 Kn_0\right) p/p_0} - \frac{2C_1 Kn_0 \left(1 + 24 C_1 Kn_0\right)}{1 + 8 C_1 Kn_0} \right.\\ &\left. \frac{1}{4}\log \frac{1 + 8C_1 Kn_0}{p/p_0 + 8 C_1 Kn_0} - \frac{3}{4}\log\left(\frac{p}{p_0}\right)\right] = -64\,\mathrm{Re}\,\beta \frac{z - z_0}{D}\end{aligned} \tag{40}$$

Sreekanth (1969) also performed detailed experiments to determine the pressure variation in a polished brass tube of 5.08 cm inner diameter and three different lengths (24.23 cm, 49.07 cm and 76.35 cm). The measurements are in the Knudsen number range of 0.012 to 0.3. The experimental data compared well with the analytical solution. Tison (1993) presented extensive measurements; his data has been utilized in subsequent studies for benchmarking. Demsis et al. (2010b) performed pressure-drop measurements for low-pressure flow of gas in a tube. The ranges of Knudsen number and Reynolds numbers covered in their study are 0.0022–0.024 and 0.54–13.2, respectively. They studied the effect of change in pipe material and channel geometry for three different gases (nitrogen, oxygen and argon). They reported that the friction factor value responds to changes in gas, tube material and geometry of cross-section.

Celata et al. (2007) performed measurements in smooth microtubes of four diameters (254, 101, 50, 30 micron, L/D varies from 300–2400). Their Reynolds number varied between 0.8–500, Knudsen number varied between 0.0003–0.0064, and the pressure ratio between 1.1 and 10. The results were presented in terms of Poiseuille number versus Reynolds number. They found that the Poiseuille number for isothermal and adiabatic conditions differed by less than 1%, suggesting that viscous heating effects are negligible. This demonstrates that both isothermal and adiabatic approximations are valid for such flows. They further concluded that the compressibility and rarefaction effects are negligible for the conditions tested. Shinagawa et al. (2002) performed conductance measurements of nitrogen gas over a large range of length to diameter ratio and pressure ratio across the tube. They also performed DSMC calculations at high Knudsen numbers. The data was compared against Hanks-Weissberg's equation. Araki et al. (2002) measured the friction constant for flow of nitrogen, helium and argon gases through quartz glass tubes of diameter ranging from 5 to 100 μm. They found a decrease in friction constant as compared to conventional sized tubes and attributed this decrease to the compressibility and rarefaction effects. They also found that the amount of decrease is larger for nitrogen (7.8%) as compared to helium (3.1%) and argon (1.56%) for tube diameter of 100 μm. Choi et al. (1991) measured the friction constant for nitrogen flow and reported that the measured values are up to 20% smaller than those predicted by the correlations for macrotubes. Du et al. (2000) performed measurements in microtubes whose diameters range from 80.0 to 166.6 micron. Their measurements suggested that the product of Fanning friction factor and Reynolds number in microtubes is same as that predicted by Moody chart when the average Mach number is less than 0.3; however the product became larger and increases with increasing average Mach number, when $Ma > 0.3$. Marino (2009) performed measurements for flow in single tubes and a bundle of capillaries over a wide range of Knudsen number. The results were compared with existing experimental data and analytical models.

Li et al. (2009) experimentally studied the flow characteristics of nitrogen in PEEK polymer microtube with a hydraulic diameter of 553 μm. They suggested that the flow transition occurs at Reynolds number ranging from 1600–2000. Transition of flow from laminar to turbulence has also been investigated by Morini et al. (2007). Morini et al. (2006) performed measurements for flow of nitrogen in commercial stainless steel microtubes of inner diameter 762, 508, 254 and 127 microns. Their results suggested that no early transition to turbulence occurs; instead the transition takes place at Reynolds numbers ranging between 1800 and 2900. They emphasized that one should measure the inner diameter of the microtubes and not just rely on the value given by the supplier. The measurements of Du et al. (2000) suggest transition at Re = 2300, which is consistent with the continuum value.

Zhao (2001) solved the compressible N-S equations for flow in a microtube. The length of the tube is assumed to be 40 times its diameter. The first-order slip with complete accommodation is used as the boundary condition. The inlet Reynolds number and inlet Mach number (for compressible flow) were taken as 0.015 and 0.001 respectively. The value of $f.\mathrm{Re}$ in their simulation varies from the value of 63.74 (at $Kn = 0.001$) to 46.93 (at $Kn = 0.1$) to 21.35 (at $Kn = 1$). Varoutis et al. (2009a) performed DSMC computations for flow in tubes. They investigated the effect of gas rarefaction, length-to-radius ratio, and pressure ratio along the tube on the flow characteristics. Asako et al. (2005) solved the compressible form of N-S equations with no-slip boundary condition (together with temperature equation) using the arbitrary-Lagrangian-Eulerian method. They also performed experiments in a 150 micron microtube. They suggested the following variations of Darcy and Fanning friction factors:

$$f_f \,\mathrm{Re} = 64 + 2.703Ma + 93.89Ma^2 \tag{41}$$

$$f_d\,\mathrm{Re} = 64 - 11.99Ma + 263.7Ma^2 \tag{42}$$

Note that because of the use of no-slip boundary condition, these correlations are not dependent on Knudsen number. Taheri and Struchtrup (2010) presented a unified theoretical approach based on the linear form of regularized 13-moment (R13) equations.

Valougeorgis (2007) suggested the following correlation based on a theoretical analysis:

$$f\,\mathrm{Re} = \frac{64}{\left[1+\left(\frac{2-\alpha}{\alpha}\right)\frac{4\sqrt{\pi}}{\delta}\right]} = \frac{64}{\left[1+\left(\frac{2-\alpha}{\alpha}\right)8Kn\right]} \tag{43}$$

Verma et al. (2009) analyzed the experimental data of Brown et al. (1946), Sreekanth (1969), Choi et al. (1991), Ewart et al. (2006, 2007a,b), Tang et al. (2007) for smooth circular tube, along with their own data. They arrived at the following correlation based on this compilation of data:

$$f\,\mathrm{Re} = \frac{64}{1+14.9Kn}. \tag{44}$$

They noted that out of 233 data points analyzed, 226 points (or 97% of the data) lie within an error band of ± 20%. The mean absolute error for the entire data set is 7.96%.

6. OTHER CROSS-SECTION MICROCHANNELS

Shapes other than rectangular and circular can be encountered in practical situations. Therefore several other shapes have been studied in the literature, although not to the same extend as the planar, rectangular and circular geometries. For example, isosceles triangular and trapezoidal microchannels considered in this section can be formed by wet etching.

6.1. Elliptical microchannel

Graur and Sharipov (20008) obtained the solution for gas flow in elliptical microchannel, over the entire range of Knudsen number. The bulk velocity in the slip region is obtained as the summation of hydrodynamic and slip-correction solutions. Whereas the hydrodynamic solution satisfies the Stokes equation, the slip velocity correction is obtained as the solution of the Laplace equation. The slip velocity at the wall is obtained as the gradient of the hydrodynamic velocity. The linearized Boltzmann equation is solved for flow in the free-molecular and transition flow regimes. The BGK model and assumption of small pressure gradient are invoked for simplifying the solution procedure. It was noted that the flow rate does not tend to the value corresponding to the parallel plates at any finite value of the rarefaction parameter, although it does so in the hydrodynamic limit of zero Knudsen number. It was suggested that the flow rate becomes dependent on the conditions over the entire cross section because of which the influence of the small curvature becomes significant in the transition and free molecular regimes.

Duan and Muzychka (2007) solved the simplified N-S equation. They argued that only the viscous and pressure terms need to be retained. The simplified equation was solved analytically using the slip boundary condition and the following expression for mass flux was obtained:

$$\dot{m} = \rho\bar{u}A = \frac{\pi a b p_o^2\left(\frac{\pi b}{E(e)}\right)^2}{8\mu Po_c RTL}\left[\frac{p_i^2}{p_o^2} - 1 + 2\alpha\frac{2-\alpha}{\alpha}Kn_o\left(\frac{p_i}{p_o} - 1\right)\right] \tag{45}$$

They further showed that slipping allows extra fluid mass to be transported across the microchannel. This extra mass can be related to no-slip mass as

$$\frac{\dot{m}}{\dot{m}_c} = 1 + \frac{2\alpha\left(\frac{2-\alpha}{\alpha}\right)Kn_o}{\frac{p_i}{p_o}+1}. \tag{46}$$

6.2. Triangular and trapezoidal microchannels

Naris and Valougeorgis (2007) solved for rarefied fully developed flow of a gas through a duct of a triangular cross section, subjected to Maxwell diffuse boundary conditions. The results are claimed to be valid in the whole range of Knudsen number. The accuracy of the solution was checked for their recovery of the analytical solutions at the free molecular and hydrodynamic limits. Shojaeian and Dibaji (2010) performed numerical calculations for steady state, laminar, incompressible, constant fluid properties flow in triangular microchannel with aspect ratio between 0.2–4.5. The effect of Knudsen number ($0.001 < Kn < 0.1$) and Reynolds number ($1 < \mathrm{Re} < 15$) on the fluid flow were studied as part of this work. Ritos et al. (2011) and Szalmas and Valougeorgis (2010) solved for flow through long microchannels with triangular and trapezoidal cross-sections. The kinetic equations are solved in the whole range of the Knudsen number.

Varoutis et al. (2009b) performed measurements of fully developed rarefied gas flows through channels of circular, orthogonal, triangular, and trapezoidal cross-sections. The channels were made out of stainless steel with a length equal of 1277 mm and a hydraulic diameter of approximately 16 mm (so that a length to diameter ratio of 80). The kinetic equation subject to Maxwell boundary conditions with diffuse and specular boundary conditions was also solved. The analysis is general, and it may be applied to channels of any cross-section. The computed and measured mass flow rates and conductance are in very good agreement in all cases investigated. Interestingly, the Knudsen minimum is always about 1 but the value differs with cross-section. Further, in some cases the Knudsen minimum is deep (orthogonal channel), while it is shallow in shallow for circular channel.

6.3. Miscellaneous shapes

Shams et al. (2009) performed simulations for flow in rhombus shaped microchannel using a commercial code. The variation of velocity profile, Poiseuille and Nusselt numbers were presented as a function of channel aspect ratio and Knudsen number. Breyiannis et al. (2007) considered flow of rarefied gas through circular ducts of concentric annular cross-section. They solved the kinetic equations for fully developed flow. The accuracy of the results was checked by examining the solutions at the hydrodynamic and free molecular limits. Duan and Muzychka (2007) proposed a model to predict the Poiseuille number for non-circular microchannels.

Stevanovic (2007) solved analytically for two-dimensional, isothermal, compressible and subsonic gas flow in a microchannel with slowly varying cross-section. The Burnett momentum equation was solved using perturbation method. It was shown the Burnet equation has the same form as the Navier–Stokes equation for low Mach number flows. The obtained analytical results agreed well with available measured data and numerical solutions of the Boltzmann equation. Xue et al. (2001) solved the micro-Couette flow using Burnett equations. Zahid et al. (2007) considered the micro-Couette flow problem with an imposed pressure gradient. Shokouhmand et al. (2011) numerically solved for flow in a constricted microchannel.

7. SURFACE ROUGHNESS

In the above sections, smooth microchannels have been considered. The effect of surface roughness on rarefied gas flow through microchannel is now presented. Nikuradse (1933) and Moody (1944) originally studied the effect of roughness on laminar flow. Richardson (1973) suggested that surface roughness affects the boundary conditions of fluid flow. He argued that the no-slip boundary condition is a consequence of the wall surface roughness for continuum fluid. Note that the flow in microchannel is often laminar.

Wu and Little (1983) experimented for gas (nitrogen, helium and argon) flow in trapezoidal microchannels with hydraulic diameters ranging from 30 to 60 micron and relative surface roughness between 0.05 and 0.30. The experimental values for the friction factor normalized with respect to the theoretical values are observed from 1.3 times higher in silica channel to 3–5 times higher in glass channels. It is noted that the higher friction factor is due to the variation of the flow cross-section caused by the large roughness. Volkov (1988) investigated slip coefficient for rough surface using Monte Carlo simulations and revealed a decrease in slip of gas flows for progressively higher surface roughness. The molecular dynamics simulation was employed by Mo and Rosenberger (1990) for 2D fluid flow through channel with sinusoidally and randomly roughened walls. They found that the no-slip condition arises when the molecular mean free path is comparable with the surface roughness amplitude. It is suggested that the ratio of mean free path to roughness amplitude should be considered to validate the no slip condition, rather than the Knudsen number. Choi et al. (1991) conducted measurements on fused-silica smooth micro-tubes (diameters ranged from 3 to 81micron) with nitrogen gas as the test fluid. The authors observed that the friction factor is not influenced by the roughness of the micro-tubes. Sugiyama et al. (1996) studied experimentally (nitrogen gas) and theoretically (Monte Carlo method) the effect of surface roughness on the conductance of passages composed of two flat plates with passage height from 0.99 to 1 mm and roughness of 4.48 to 16.46 micron. The two dimensional roughness of triangular wave of constant amplitude is cut on plates by machining process. It is observed that the conductance decreases with the increase in the angle of triangular wave, and the effects of the angle become considerable at larger inverse Knudsen numbers. Guo and Li (2003) noted that the surface roughness is responsible for the early transition from laminar to turbulent flow and the increased friction factor. The DSMC results for nitrogen flow in a microchannel with surface roughness modeled by an array of rectangular modules that are placed uniformly on two surfaces of a parallel plate channel are presented by Sun and Faghri (2003). It is observed that (Fig. 8) friction constant increases significantly as the relative roughness increases from 2 to 6%.

Turner et al. (2004) presented experimental investigation of the effect of surface roughness on friction factor. The friction factor is determined experimentally using rectangular silicon microchannel (surface roughness e = 0.0082 to 1.62 micron, relative roughness e/H = 0.004 to 0.03) with helium and nitrogen gas. The effect of the relative surface roughness on the friction factor is found within 2–6 percent. It is concluded that the effect of surface roughness on the friction factor is insignificant for both continuum and slip flow regimes. The molecular dynamics simulation by Cao et al. (2006) is used to investigate the effect of surface roughness on slip flow of argon in platinum channels. The surface roughness (relative roughness from 0.6 to 4.8%) is modeled by triangular (Cao et al. 2004), rectangular, sinusoidal and randomly triangular waves respectively. It is noted that friction coefficient increases

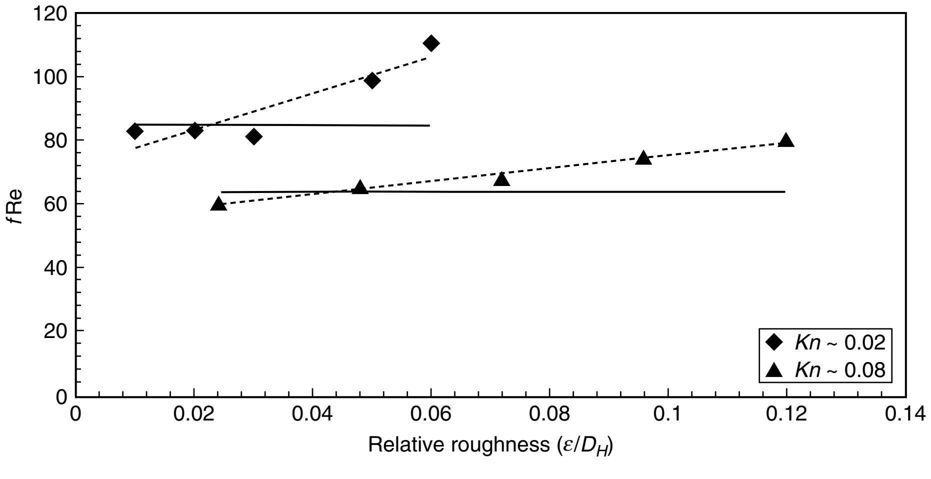

Figure 8. Effect of relative roughness on fRe value. [from Sun and Faghri (2003)]

with increasing surface roughness and the slip length over the rough surface is less than that from Maxwell's slip model. Further, Cao (2007) investigated rarefied gas flows in rough microchannels using non-equilibrium molecular dynamics simulations. The surface roughness is modelled by an array of triangular modules. It is found that the Maxwell slip model break down due to the surface roughness for gas flows in microchannels with large surface roughness. It is noted that permeability due to surface roughness is responsible for the non-Maxwell slippage. It is suggested that penetrating and multi collisions of molecules near a rough surface is the reason for the breakdown of the bounce-back assumption used by the Maxwell theory. The numerical simulation for 2D compressible gas flow through a microchannel in the slip regime by Ji et al. (2006) indicates that the average Poiseuille number increases as the roughness height is increased and as the spacing distance between the roughness elements is decreased. Croce et al. (2007) presented a numerical analysis of rarefied compressible flow in a plane microchannel with saw-tooth shaped roughness ribs (relative roughness from 0 to 2.65%). It is observed that for moderately rarefied flow the pressure drop in rough channels is higher than that predicted by standard macroscale correlations. The pressure drop increase is around 20% for a roughness of the order of 2–3%. Zhang and Jia (2007) investigated numerically the effect of surface roughness on friction factor for nitrogen flow through rectangular channel of 100 micron hydraulic diameter. The roughness is modeled as regular obstructions placed on the channel walls. It is noted that friction factor increases with an increase in roughness height. Tang et al. (2007) studied experimentally for nitrogen and helium gas flow through fused silica microtubes with diameters from 50 to 201 micron and fused silica square channels with hydraulic diameter from 52 to 100 micron. In the fused silica microtubes and microchannels friction factors are in good agreement with the theoretical predictions whereas the friction factors in stainless steel tubes (diameter 119 to 300 micron) are much higher than the theoretical predictions. The increase in friction factor is accounted to the dense roughness distribution in the inner surface of the stainless steel tubes. The lattice Boltzmann method is used by Chai et al. (2008) to investigate the gaseous flow in a microchannel with surface roughness modeled by an array of rectangular modules. It is found that increase in relative roughness and roughness distribution increases friction factor and decreases mass flow rate. Ziarani and Mohamad (2008) investigated the effect of wall roughness on the slip in microchannel using molecular dynamics simulation. The negative slip is observed for surfaces with larger amplitudes of roughness. The negative slip is justified by backflow between rough elements. The nitrogen gas flow through circular microchannel of diameter from 26 to 508 micron with different surface roughness is investigated experimentally by Lorenzini et al. (2009). It is observed that in the laminar regime the friction factor is in agreement with conventional theory for rough and smooth microtubes. Khadem et al. (2009) simulated wall roughness with periodically distributed triangular microelements and random shaped micro peaks distributed on the wall surfaces. It is observed that the rough elements cause more pressure drop and increases in the Poiseuille number due to the obstruction effect. Liu and Ni (2009) studied the fractal roughness effect of 2D helium and nitrogen gas flow using modified lattice Boltzmann model. It is noted that the relative resistance coefficient increases as the relative roughness increases and the resistance coefficient of nitrogen is found larger than that of helium at a same roughness. Ghajar et al. (2010) experimented with nitrogen gas flow through microtubes (one glass tube and 5 stainless steel tubes with inner diameter from 1000 to 2000 microns) with roughness from 0 to 4.3 microns and relative roughness (ε/D) from 0 to 0.004308. It is observed that the range of transition Reynolds number was narrower with the increase of surface roughness. Demsis et al. (2010b) studied experimentally the effect of pipe wall roughness on friction factor for gas flow through circular and square pipe with stainless steel and copper material. It is observed that (Fig. 9) an increase in relative roughness from the standard value of 0.2% to 0.5% and 1% results in an increase in the friction constant as 10% and 13%, respectively, for nitrogen.

It is clear from the review that many researchers observed marginal increase in friction factor (around 4–6% higher except Wu and Little, 1983 for glass channel and Demsis et al. 2010b) than conventional due to increase in surface roughness. Considering experimental uncertainty the noted increase in friction factor seems insignificant and surface roughness may be neglected. We recognize the need for more detail and accurate investigations in this context.

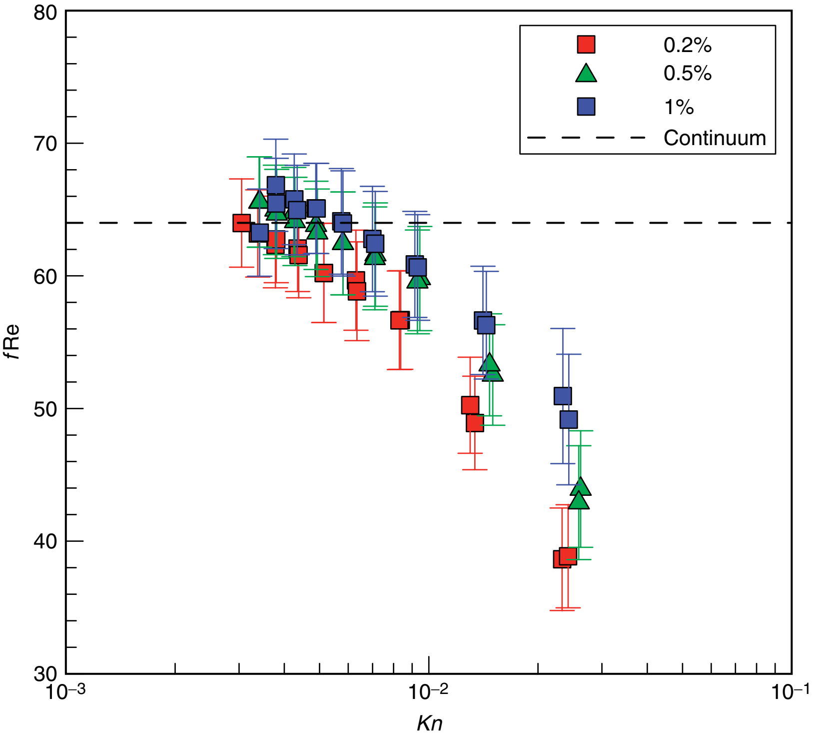

Figure 9. Effect of Roughness in slip regime for Nitrogen. [from Demsis et al. (2010)]

8. REVIEW ON COMPLEX MICROCHANNELS

In most practical applications microchannels are not straight and the area cross section is not constant due to sudden contraction or expansion. Bends, T's, Y's, expansions and contractions are common features of micro systems. The work carried out by various researchers on gas flow through such complex microchannels is reviewed in this section.

8.1. Microchannel with bend

We first consider flow in a bend. Lee et al. (2001) experimentally investigated gas flow in a microchannel; their pressure measurements (see Fig. 10) indicate that secondary flow could develop in microchannels in the vicinity of the bend. An experimental study on rarefied gas flow through a single 90° bend in the slip flow regime is presented by Varade et al. (2010). They employed nitrogen at low pressure in conventional tubes to achieve relatively large Knudsen number. The adverse pressure gradients are observed near the bend at a small Reynolds number of 3.3 which is noted as an indication of separation at the bend.

Maharudrayya et al. (2004) computed the pressure loss coefficient across the bend as a function of Reynolds number, aspect ratio, curvature ratio and spacer length for incompressible flow of air. The flow separation is observed at the inner wall of the bend at Re = 100 and at Re = 200 at the outer wall, while there is no flow separation for Re < 50. The microchannel gas flow through a sharp 90° bend was analyzed by Wang and Li (2004) using a modified DSMC code. It was observed that there is an increase in pressure at the bend but separation is not noted at the bend. The larger pressure loss is related to flow aspects. Raghavan and Premchandran (2008) numerically investigated the effect of fillet radius on gas flow through microchannel with a right-angle bend. It is observed that flow separation occurs after the bend for zero fillet radius. Agrawal et al. (2009) used the lattice Boltzmann method to study flow of gas through microchannels with a single 90° bend. They noted that velocity and pressure distribution between the bend and straight channel are identical away from the bend at large Knudsen numbers.

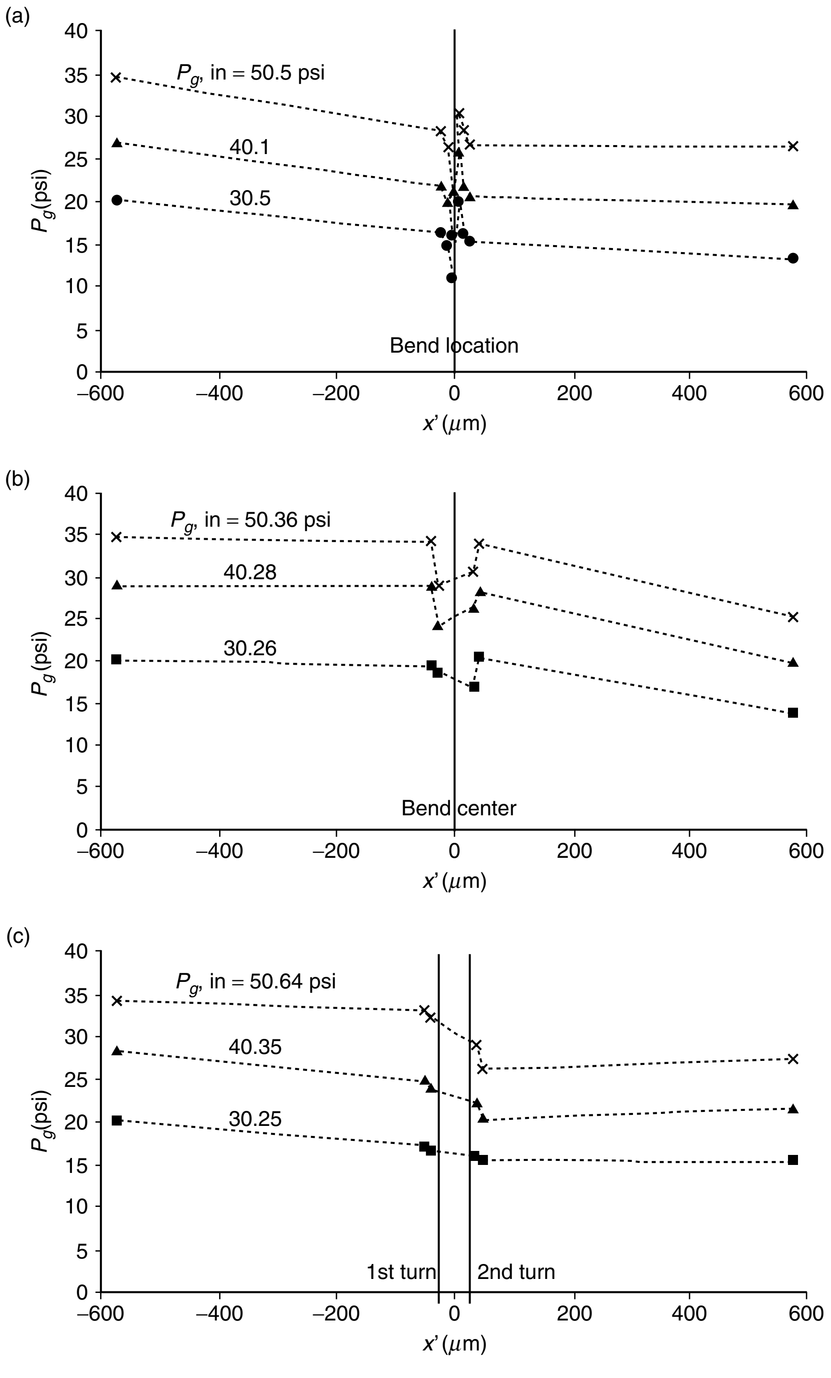

Figure 10. Detailed pressure distribution along the inner wall of the (a) miter, (b) curved, and (c) double-turn bends. [from Lee et al. (2001)]

Their investigation suggests the presence of secondary flow near the bend even for small Reynolds number (Re ≈ 0.3) (Fig. 11). Croce and Rovenskaya (2010) provided 3D Navier-Stokes solution with first order slip boundary condition and analyzed the effect of channel aspect ratio, bend curvature, rarefaction and compressibility. It is claimed that the effect of the bend on the channel global performances is minimum at higher rarefaction. Raju and Roy (2003) numerically studied two 90°

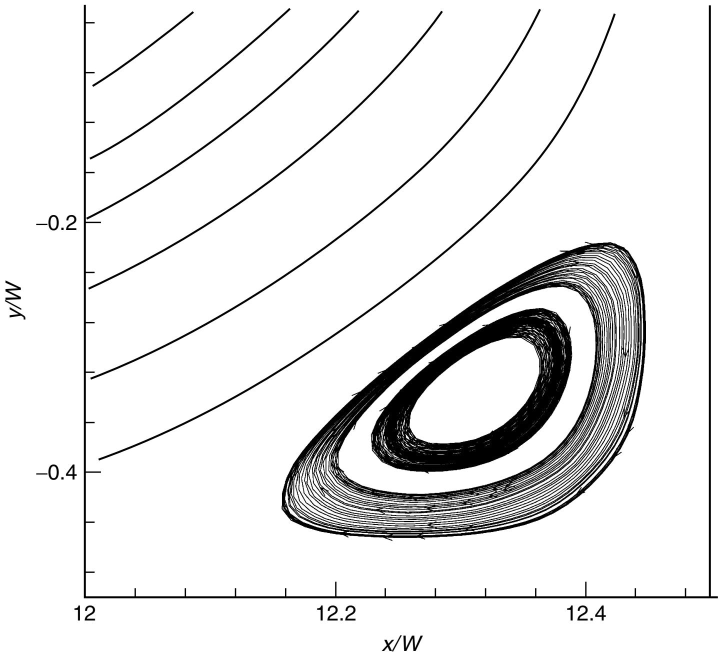

Figure 11. Zoomed view near the bend, showing folded streamlines and presence of an eddy at the corner for *Kn* = 0.060 (Re = 19.33). [from Agrawal et al. (2009)]

bends. They reported that the mass flow rate in bend microchannel is lower by 60% as compared to a straight channel for the same pressure ratio across the channel with the same overall dimensions of the two microchannels.

In summary, experimental and numerical investigation by many researchers (except Wang and Li, 2004; Croce and Rovenskaya, 2010) suggests that flow separation occurs at the bend for a laminar microchannel gas flow. The higher pressure drop than straight microchannel is owing to this separation at the bend.

8.2. Microchannel with sudden expansion/contraction

Change is cross-section area is frequently encountered. In this section, we review literature on flow through sudden expansion or contraction. Lee et al. (2002) experimentally investigated gas flow through microchannels connected via a transition section with included angle varying from 0° to 180° using nitrogen gas. They observed that the measured mass flow rate decreases and the pressure loss increases with increasing included angle of the transition section. Rathakrishnan and Sreekanth (1994) presented experimental results on rarefied gas flow through sudden enlargements. It is noted that the discharge is a strong function of the ratio of the enlargement diameter to inlet tube diameter.

The numerical solutions (DSMC and Navier-Stokes solution with higher order slip boundary condition) of rarefied gas flow through microchannels with backward-facing step geometry are presented by Beskok (2001). The flow separation at the sudden expansion is predicted for Re = 80, $Kn_0 = 0.04$, $Ma = 0.45$. Beskok (2001) showed that the non-dimensional separation distance reduces as the Knudsen number at the step expansion increases. Agrawal et al. (2005) developed two dimensional simulations based on isothermal lattice Boltzmann method, applicable to microchannels with a sudden expansion or contraction. It is noted that for the diverging geometry there is no flow separation at the corner and vena contracta is not observed for converging geometry. They further postulated that flow in complex geometries can be obtained as solution in their primary units (Fig. 12). Yan et al. (2008) simulated nitrogen gas flow through sudden expansion and contraction by DSMC method in both slip and transition regimes. It is observed that the resistance coefficient for the microchannel is much smaller than conventional-scale channels.

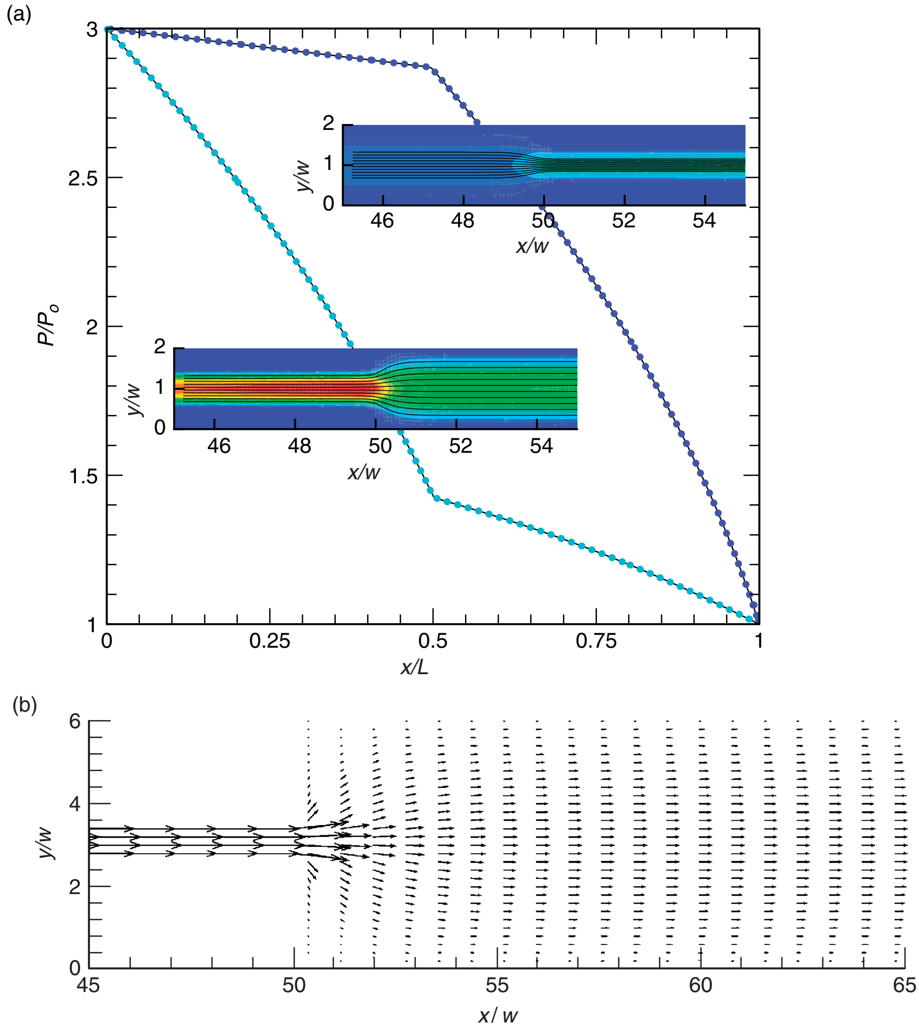

Figure 12. (a) Comparison of pressure between simulations (line) and theory of Arkilic et al. (1997) (dots) for the converging (top curve) and diverging (bottom curve) microchannels. The Knudsen numbers at the outlet are 0.012 and 0.0074 for the converging and diverging microchannels, respectively. Streamlines for diverging and converging microchannels superposed with contours of the streamwise velocity are shown as inset to the figure. The streamlines are reminiscent of potential flows. The *x*- axis is normalized by the microchannel length and pressure (on *y*-axis) by exit pressure (p_o). (b) Vector field for a diverging microchannel with area-ratio of six. The number of vectors has been substantially reduced in order to avoid overcrowding the figure. The *x*- and *y*-axes are normalized by the width (*w*) of the microchannel. [from Agrawal et al. 2005]

8.3. Gas flow through micro-filter

We now briefly consider flow through micro-filter as an application. Saxena et al. (2009) designed, fabricated and tested micro-filters containing up to 14000 holes. The mean pore size on the fabricated micro-filters is 14.4 μm, 18.3 μm and 25.6 μm. The pressure drop with air as the fluid was measured and the data compared with the correlation of Yang et al. (1999; 2001) and Mott et al. (2001). However, substantial deviation was noted because of which they proposed the following modified correlation.

$$\frac{\Delta p}{\frac{1}{2}\rho U^2} = 0.0009893\beta^{-2}\left(3.5\frac{t}{d}+3\right)^{6.337}\left(\frac{10}{\mathrm{Re}}+0.22\right)^{0.5915}. \tag{47}$$

Kamali and Binesh (2009) solved for flow between two half-square bodies, with application to micro-filters. Czerwinska and Jebauer (2011) solved for flow around two fixed cylinder objects located in a microchannel, in steady low Reynolds number and low Knudsen number ($\mathrm{Re} \ll 1$; $Kn \ll 0.1$) regime. The effect of slip on vorticity generation from the cylindrical surfaces was investigated. Fissell et al. (2011) experimentally studied gas flows over a wide range of Knudsen numbers (0.5–10) using silicon nanochannel arrays with slit-shaped pores. Raju and Kurian (1994) also present measurements through rectangular slit.

9. CONCLUSIONS AND DIRECTIONS FOR FUTURE WORK

A review of gas flow in microchannels of different cross-sections is presented in this article. The phenomenon of slip, slip models and measurement of slip coefficient are first discussed. A number of slip models have been proposed in the literature; however, most of them have not been rigorously tested. It is noted that effect similar to slipping can be obtained by alternate means, such as by employing either effective viscosity near the wall or solving extended Navier-Stokes equations with no-slip boundary condition.

The article deals in great detail with planar microchannels where a large number of analytical, experimental and simulation approaches and solutions are available. Analytical solutions obtained by different approaches agree reasonably well amongst each other. Availability of good quality experimental data (in terms of streamwise pressure variation with reasonable resolution) and analytical solution has facilitated the development of various numerical schemes. A large number of studies have focused on enhancing the capability of DSMC and LBM to accurately simulate flow in the slip and transition regimes.

Review of studies on square, rectangular and circular microchannels have revealed that these microchannels have also been extensively considered. Analytical solution and numerical/ experimental data for such microchannels is available. Information on other shapes of microchannels which can be fabricated such as triangular and trapezoidal is also presented.

The case of surface roughness is given due attention; it is felt that more detailed and precise measurements with different surface materials and conditions is required. It is further recognized that frequently the microchannels may not be straight; therefore, microchannels with bends or involving sudden expansion/ contraction is considered. Gas flow across a micro-filter is briefly mentioned as an application.

The following are some suggestions for future research directions in this field:

1. Maxwell slip model has been extensively applied in the literature. However, the condition and parameter range over which it is valid, needs to be rigorously established.
2. Data for TMAC with nonmonatomic gases needs to be generated as these gases are more commonly encountered in practical situations as compared to noble gases, which have been the focus of earlier investigations.
3. The effect of surface roughness on TMAC and Poiseuille number needs to be unambiguously established.
4. The flow near an impenetrable wall (example micro-duct) will have two velocity components in general. The slip of the lateral velocity component has not received attention in the literature and can be investigated in future studies.
5. Although data for streamwise variation in pressure is available, the same is not true with other quantities such as velocity components and wall shear stress. Measurement of these quantities can help develop better slip models besides serving as benchmark for theoretical analysis and numerical simulations.
6. Although correlations to calculate the friction factor for some simple cross-sections (planar, square and circular) are available, such correlations need to be developed and rigorously tested for other cross-sections.

7. There is enough scope to study various complex microchannels. In any application, microchannels will not be straight. Such a study therefore holds great practical importance.

ACKNOWLEDGEMENT

Section 7 of this article was primarily prepared by Mr. Vijay V. Varade. I am grateful to Mr. Varade and Mr. Vijay S. Duryodhan for their help in completing this article. Funding from ISRO-IITB cell and IIT Bombay is acknowledged.

REFERENCES

[1] Agarwal R. K., Yun K. Y. & Balakrishnan R., Beyond Navier–Stokes equations for flows in the continuum-transition regime. Phys. Fluids 10, 3061–3085, (2001).

[2] Agrawal A., and Agrawal A., Three-dimensional simulation of gas flow in microduct. ASME 3rd International Conference on Microchannels and Minichannels (ICMM2005) June 13–15, Toronto, Ontario, Canada, Paper no. ICMM2005-75023, 369–376, (2005).

[3] Agrawal A. and Agrawal A., Three-dimensional simulation of gaseous slip flow in different aspect ratio microducts, Physics of Fluids, Vol. 18 (103604), 1–11, (2006).

[4] Agrawal A., Djenidi L. and Agrawal A., Simulation of gas flow in microchannels with a single 900 bend, Computers & Fluids, 38, 1629–1637, (2009).

[5] Agrawal A., Djenidi L. and Antonia R.A., Simulation of gas flow in microchannels with a sudden expansion or contraction, Journal of Fluid Mechanics, 530, 135–144, (2005).

[6] Agrawal A. and Dongari N., Application of Navier-Stokes equations to high Knudsen number flow in a fine capillary, International Journal of Microscale and Nanoscale Thermal and Fluid Transport Phenomena, to appear, (2011).

[7] Agrawal A, and Prabhu S.V., Deduction of slip coefficient in slip and transition regime from existing cylindrical Couette flow data. Experimental Thermal and Fluid Sciences 32, 991–996, (2008a).

[8] Agrawal A, and Prabhu S.V., Survey on measurement of tangential momentum accommodation coefficient. Journal of Vacuum Science Technology A 26 (4), 634–645, (2008b).

[9] Ahmed N.K. and Hecht M., A boundary condition with adjustable slip length for lattice Boltzmann simulations, Journal of Statistical Mechanics, P09017, (2009).

[10] Alexander F.J., Garcia A.L. and Alder B.J., A consistent Boltzmann algorithm, Phys. Rev. Lett., 74, 5212, (1995).

[11] Ansumali S. and Karlin I. V., Kinetic boundary conditions in the lattice Boltzmann method, J. Stat. Phys., 107, 291, (2002).

[12] Ansumali S., Karlin I.V., Frouzakis C.E., Boulouchos K.B., Entropic lattice Boltzmann method for microflows. Physica A 359, 289–305, (2006).

[13] Aoki K., Takata S. and Nakanishi T., Poiseuille-type flow of a rarefied gas between two parallel plates driven by a uniform external force. Physical Review E, 65, 026315, (2002).

[14] Araki T., Kim M.S., Iwai, H. and Suzuki K., An experimental investigation of gaseous flow characteristics in microtubes. Microscale Thermophysical Engineering, 6(2), 117–130, (2002).

[15] Arkilic E.B., Schimidt M.A. and Breuer K.S., Gaseous slip flow in long micro-channels, J. Microelectromech. Syst. 6, 167–178, (1997).

[16] Arkilic E.B., Breuer K.S. and Schimidt M.A., Mass flow and tangential momentum accommodation in silicon micromachined channels, J. Fluid Mech. 437, 29–43, (2001).

[17] Arlemark E.J., Dadzie S.K. and Reese J.M., An extension to the Navier-Stokes equations to incorporate gas molecular collisions with boundaries. Journal of Heat Transfer, 132 (4), (041006) 1–8, (2010).

[18] Asako Y., Nakayama K. and Shinozuka T., Effect of compressibility on gaseous flows in a micro-tube. International Journal of Heat and Mass Transfer, 48, 4985–4994, (2005).

[19] Bao F. and Lin J., Burnett simulations of gas flow and heat transfer in microchannels. Front. Mech. Eng. China, 4(3), 252–263, (2009).

[20] Bao F. and Lin J., Burnett simulations of gas flow in microchannels. Fluid Dynamics Research 40, 679–694, (2008).

[21] Bentz, J.A., Tompson, R.V., and Loyalka, S.K. Measurements of viscosity, velocity slip coefficients, and tangential momentum accommodation coefficients using a modified spinning rotor gauge. Journal of Vacuum Science and Technology A, 19, 317–324 (2001).

[22] Bentz, J.A., Tompson, R.V., and Loyalka, S.K. The spinning rotor gauge: Measurements of viscosity, velocity slip coefficients, and tangential momentum accommodation coefficients for N2 and CH4, Vacuum, 48, 817–824 (1997).

[23] Benzi R., Succi S. and Vergassola M., The lattice Boltzmann equation: theory and applications, Phys. Rep., 222 (3),145–197, (1992).

[24] Beskok A. and Karniadakis G.E., A model for flows in channels, pipes, and ducts at micro and nano scales. Microscale Thermophysical Engineering 3, 43–77, (1999).

[25] Beskok A., Karniadakis G.E. and Trimmer W., Rarefaction and Compressibility Effects in Gas Microflows, J. Fluids Eng., 118, 448–456, (1996).

[26] Beskok A., Validation of a new velocity-slip model for separated gas microflows, Numerical Heat Transfer B, 40, 451–471, (2001).

[27] Bhatnagar P. L., Gross E. P. and Krook M., A Model for Collision Processes in gases. I. Small Amplitude Processes in Charged and Neutral One-Component Systems, Phys. Rev., 94, 511–525, (1954).

[28] Bird, G. A., Molecular Gas Dynamics and the Direct Simulation of Gas Flows, Oxford University Press, New York, (1994).

[29] Blanchard D. and Ligrani P, Slip and accommodation coefficient from rarefaction and roughness in rotation microscale disk flows, Physics Fluids, 19, 063602, (2007).

[30] Blankenstein E, Coefficients of slip and momentum transfer in hydrogen, helium, air and oxygen, Physical Review, 22, 582–589, (1923).

[31] Brenner H, Navier-Stokes revisited. Physica A, 349, 60–132 (2005).

[32] Breyiannis G., Varoutis S., Valougeorgis D., Rarefied gas flow in concentric annular tube: Estimation of the Poiseuille number and the exact hydraulic diameter. European Journal of Mechanics B/Fluids, 27, 609–602, (2007).

[33] Brown G.P., Dinardo A., Cheng G.K. and Sherwood T.K., The flow of gases in pipes at low pressures. Journal of Applied Physics, 17, 802–813, (1946).

[34] Cai C., Boyd I.D., Fan J. and Candler G.V., Direct Simulation Methods for Low-Speed Microchannel Flows, Journal of Thermodynamics and Heat Transfer, 14 (3), 368–378, (2000).

[35] Cao B.Y., Chen M. and Guo Z.Y., Effect of surface roughness on gas flow in microchannels by molecular dynamics simulation, International Journal of Engineering Science, 44, 927–937, (2006).

[36] Cao B.Y., Chen M. and Guo Z.Y., Rarefied Gas Flow in Rough Microchannels by Molecular Dynamics Simulation, Chinese Phys. Lett., 21 (9), 1777–1779, (2004).

[37] Cao B.Y., Non-Maxwell slippage induced by surface roughness for microscale gas flow: a molecular dynamics simulation, Molecular Physics, 105, 10, 1403–1410, (2007).

[38] Cao, B.Y., Chen, M., and Guo, Z.Y. Temperature dependence of the tangential momentum accommodation coefficient for gases, Applied Physics Letters, 86, 091905, (2005).

[39] Celata G.P., Cumo M., McPhail S.J., Tesfagabir L., Zummo G., Experimental study on compressible flow in microtubes. International Journal of Heat and Fluid Flow, 28, 28–36, (2007).

[40] Cercignani C. and Daneri A., Flow of a rarefied gas between two parallel plates, J. Appl. Phys. 34, 3509–3513, (1963).

[41] Cercignani C., Lampis M. and Lorenzani S., Variational approach to gas flows in microchannels, Phys. Fluids, 16, 3426–3437, (2004)

[42] Cercignani C., Lampis M., Kinetic models for gas–surface interaction, Transport Theory Statistical Physics, 1, 101, (1971).

[43] Cercignani Carlo and Lorenzani S., Variational derivation of second-order slip coefficients on the basis of the Boltzmann equation for hard-sphere molecules. Physics of Fluids 22, 062004 (2010).

[44] Chai Z., Guo Z., Zheng L., and Shi B., Lattice Boltzmann simulation of surface roughness effect on gaseous flow in a microchannel, Journal of Applied Physics, 104, (014902) 1–8, (2008).

[45] Chakraborty S. and Durst F., Derivations of extended Navier–Stokes equations from upscaled molecular transport considerations for compressible ideal gas flow: towards extended constitutive forms, Phys Fluids, 19 (088104), 1–4, (2007).

[46] Chapman, S., Cowling, T.G., The Mathematical Theory of Nonuniform Gases. Cambridge University Press, New York, (1970).

[47] Chen Sheng, Tian Zhiwei, Simulation of microchannel flow using the lattice Boltzmann method. Physica A 388, 4803–4810, (2009).

[48] Chew, A.D., Chambers, A., and Troup, A.P. The gas species dependence of the performance of a rotating disc absolute pressure gauge in high vacuum. Vacuum, 44, 583–585 (1993).

[49] Choi S. B., Barron R. F., and Warrington R. O., Fluid Flow and Heat Transfer in Micro-tubes, Proceedings of Winter Annual Meeting of the ASME Dynamic Systems and Control Division, Atlanta, GA, 32, 123–134, (1991).

[50] Chun J. and Koch D. L., A direct simulation Monte Carlo method for rarefied gas flows in the limit of small Mach number, Physics of Fluids, 17, 107107, (2005).

[51] Colin S., Lalonde P., and Caen R., Validation of a Second-Order Slip Flow Model in Rectangular Microchannels, Heat Transfer Engineering, 25, 23–30 (2004).

[52] Comsa G., Fremerey J.K., Lindenau B., Messer, G. and Rohl P., Calibration of a spinning rotor gas friction gauge against a fundamental vacuum pressure standard, Journal of Vacuum Science and Technology, 17, 642–644 (1980).

[53] Cooper S.M., Cruden B.A., Meyyappan, M., Raju, R., and Roy, S. Gas transport characteristics through a carbon nanotubule. Nano Letters, 4, 377–381 (2004).

[54] Croce G. and Rovenskaya O., Three dimensional effects in compressible, rarefied gas flow in bent microchannels, 2nd European Conference on Microfluidics – 2010, Toulouse, France, (December 2010).

[55] Croce G., D'Agaro P. and Filippo A., Compressibility and Rarefaction Effects on Pressure Drop in Rough Microchannels, Heat Transfer Engineering, 28 (8–9), 688–695, (2007).

[56] Czerwinska J. and Jebauer S., Secondary slip structures in heated micro-geometries. International Journal of Heat and Mass Transfer 54, 1578–1586, (2011).

[57] Demsis, A., Verma, B., Prabhu, S.V., and Agrawal, A. Experimental determination of heat transfer coefficient in the slip regime and its anomalously low value, Physical Review E 80, 016311 (2009).

[58] Demsis, A., Verma, B., Prabhu, S.V., and Agrawal, A. Heat Transfer coefficient of gas flowing in a circular tube under rarefied condition, International Journal of Thermal Sciences 49, 1994–1999 (2010a).

[59] Demsis A., Prabhu S. V. and Agrawal A., Influence of wall conditions on friction factor for flow of gases under slip condition, Experimental Thermal and Fluid Science, 34, 1448–1455, (2010b).

[60] Djordjević V., Modeling of the slip boundary condition in micro-channel/pipe flow via fractional derivative, Monograph of Academy of Nonlinear Sciences, Advances in Nonlinear Sciences II - Sciences and Applications, Belgrade, 2, 136–158, (2008).

[61] Dongari N., Agrawal A. and Agrawal A., Analytical solution of gaseous slip flow in long microchannels, Int. J. Heat Mass Transfer, 50, 3411–3421, (2007).

[62] Dongari N., Dadzie S. K., Zhang Y. and Reese J. M., Isothermal micro-channel gas flow using a hydrodynamic model with dissipative mass flux, Proc. ASME ICNMM2010 (Montreal, Canada), p 30743, (2010a).

[63] Dongari N., Durst F. and Chakraborty S., Predicting microscale gas flows and rarefaction effects through extended Navier–Stokes–Fourier equations from phoretic transport considerations, Microfluidics and Nanofluidics, 9, 831–846, (2010b).

[64] Dongari N., Sambasivam R. and Durst F., Extended Navier-Stokes Equations and Treatments of Micro-Channel Gas Flows, Journal of Fluid Science and Technology, 4 (2), 454–467, (2009a).

[65] Dongari N., Sharma A. and Durst F., Pressure-driven diffusive gas flows in micro-channels: from the Knudsen to the continuum regimes, Microfluidics and Nanofluidics, 6, 679–692, (2009b).

[66] Dongari N., Zhang Y. and Reese J.M., Modeling of Knudsen Layer Effects in Micro/Nanoscale Gas Flows. Journal of Fluids Engineering, 133, 071101, (2011).

[67] Du D., Li Z. and Guo Z., Friction resistance for gas flow in smooth microtubes. Science in China Series E: Technological Sciences, 43, 171–177, (2000).

[68] Duan Z. and Muzychka Y.S., Models for gaseous slip flow in non-circular microchannels. Proceedings of 2007 ASME-JSME Thermal Engineering Summer Heat Transfer Conference. July 8-12, Vancouver, British Columbia, Canada, (2007).

[69] Duan Z. and Muzychka Y.S., Slip flow in elliptic microchannels, International Journal of Thermal Sciences 46, 1104–1111, (2007).

[70] Durst F., Gomes, J. and Sambasivam, R., Thermofluiddynamics: Do we solve the right kind of equations? Proceeding of The International Symposium on Turbulence, Heat and Mass Transfer - Dubrovnik, Croatia, pp. 3–18, September 25–29, (2006).

[71] Ewart T., Perrier P., Graur I. and Meolans J. G., Mass flow rate measurements in gas micro flows. Experiments in Fluids, 41, 487–498, (2006).

[72] Ewart T., Perrier P., Graur I. and Meolans J. G., Tangential momentum accommodation in mirotube. Microfluidics and Nanofluidics, 3, 689–695, (2007a).

[73] Ewart T., Perrier P., Graur I. and Meolans J. G., Mass flow rate measurements in a microchannel, from hydrodynamic to near free molecular regimes. J. Fluid Mech., 584, 337–356, (2007b).

[74] Fan J. and Shen V, Statistical Simulation of Low-Speed Rarefied Gas Flows, Journal of Computational Physics, 167, 393–412, (2001).

[75] Fang Y. and Liou William W., Computations of the Flow and Heat Transfer in Microdevices Using DSMC With Implicit Boundary Conditions, J. Heat Transfer, 124, 338–345, (2002).

[76] Fissell W.H., Conlisk A. T., Datta S., Magistrelli J.M., Glass J.T., Fleischman A.J. and Roy S., High Knudsen number fluid flow at near-standard temperature and pressure conditions using precision nanochannels, Microfluid Nanofluid, 10, 425–433, (2011).

[77] Gabis D.S., Loyalka S.K., and Strovick T.S. Measurements of the tangential momentum accommodation coefficient in the transition flow regime with a spinning rotor gauge, Journal of Vacuum Science and Technology A, 14, 2592–2598 (1996).

[78] Gad-el-Hak M., The fluid mechanics of microdevices – The Freeman scholar lecture, J. Fluids Eng. 121, 5–33, (1999).

[79] Ghajar A. J., Tam L. M., Tam H. K. and Wen Q., The Effect of Inner Surface Roughness on Friction Factor in Horizontal Microtubes, 2nd International Conference on Mechanical and Electronics Engineering (ICMEE 2010), (2010).

[80] Graur I. and Sharipov F., Gas flow through an elliptical tube over the whole range of the gas rarefaction. European Journal of Mechanics B 27, 335–345, (2008).

[81] Gronych T., Ulman R., Peksa L., and Repa P. Measurements of the relative tangential momentum

accommodation coefficient for different gases with a viscosity vacuum gauge, Vacuum, 73, 275–279 (2004).

[82] Guo Z. L, Shi B.C and Zheng C.G., An extended Navier-Stokes formulation for gas flows in the Knudsen layer near a wall. Europhys Lett. 80, 24001, (2007a).

[83] Guo Z., Zhao T.S. and Shi Y., Physical symmetry, spatial accuracy, and relaxation time of the lattice Boltzmann equation for microgas flows, Journal of Applied Physics, 99, 074903, (2006).

[84] Guo Z.L. and Zheng C.G., Analysis of lattice Boltzmann equation for microscale gas flows: relaxation times, boundary conditions and the Knudsen layer. Int. J. Comput. Fluid Dyn, 22, 465–473, (2008).

[85] Guo Z.L., Shi B.C., Zhao T.S. and Zheng C.G., Discrete effects on boundary conditions for the lattice Boltzmann equation in simulating microscale gas flows. Phys. Rev. E, 76, 056704 (2007b).

[86] Guo Z.L., Zheng C.G. and Shi B.C., Lattice Boltzmann equation with multiple effective relaxation times for gaseous microscale flow. Phys. Rev. E, 77, 036707, (2008).

[87] Guo Z.Y. and Li Z.X., Size effect on microscale single-phase flow and heat transfer, International Journal of Heat and Mass Transfer, 46, 149–159, (2003).

[88] Hadjiconstantinou N. G., Comment on Cercignani's second-order slip coefficient. Physics of Fluids, 15, 2352, (2003).

[89] Harley J.C., Huang Y., Bau H.H. and Zemel J.N., Gas flow in micro-channels, J. Fluid Mech., 284, 257, (1995).

[90] Harting J., Kunert C. and Hyvaluoma J., Lattice Boltzmann simulations in microfluidics: probing the no-slip boundary condition in hydrophobic, rough, and surface nanobubble laden microchannels, Microfluidics and Nanofluidics, 8, 1–10, (2010).

[91] Hetsroni G., Mosyak A., Pogrebnyak E., Yarin L.P., Fluid flow in micro-channels. International Journal of Heat and Mass Transfer, 48, 1982–1998, (2005).

[92] Hettiarachchi H.D.M., Golubovic M., Worek W.M. and Minkowycz W.J., Three-dimensional laminar slip-flow and heat transfer in a rectangular microchannel with constant wall temperature. International Journal of Heat and Mass Transfer, 51, 5088–5096, (2008).

[93] Ho C.M. and Tai Y.C., Micro-electro-mechanical-systems (MEMS) and fluid flows, Annu. Rev. Fluid Mech. 30, 579–612, (1998).

[94] Hong C., Asako Y. and Turner S.E., Mohammad Faghri Friction Factor Correlations for Gas Flow in Slip Flow Regime, J. Fluids Eng., 129 (10), 1268–1276, (2007).

[95] Hsieh S.S., Tsai H.H., Lin C.Y., Huang C.F. and Chien C.M., Gas flow in a long microchannel, Int. J. of Heat and Mass Transfer 47, 3877–3887, (2004).

[96] Hsieh, T.-Y., Lee, T.-H., Hong, Z.-C., Yang, J.-Y., Kang, J.-H. Rarefaction effect on flow characteristics of microchannel flows. Journal of Aeronautics, Astronautics and Aviation, Series A 42 (3), 149–158, (2010).

[97] Hu G. and Li D., Multiscale phenomena in microfluidics and nanofluidics, Chemical Engineering Science 62, 3443–3454, (2007).

[98] Huang C., Gregory J.W., Sullivan J.P., Microchannel pressure measurements using molecular sensors. J. of Microelectromechanical Systems, 16 (4), 777–785 (2007a).

[99] Huang H., Lee T.S. and Shu C., Lattice Boltzmann method simulation gas slip flow in long microtubes, International Journal of Numerical Methods for Heat & Fluid Flow, 17 (6), 587–607, (2007b).

[100] Jang J. and Wereley S.T., Effective heights and tangential momentum accommodation coefficients of gaseous slip flows in deep reactive ion etching rectangular microchannels, Journal of Micromechanics and Microengineering, 16, 493–504 (2006).

[101] Jang J. and Wereley S. T., Pressure distributions of gaseous slip flow in straight and uniform rectangular microchannels, Microfluidics and Nanofluidics 1, 41 (2004).

[102] Ji Y, Yuan K, Chung J.N., Numerical simulation of wall roughness on gaseous flow and heat transfer in a microchannel, International Journal of Heat and Mass Transfer, 49, 1329–1339, (2006).

[103] Kamali R., Binesh A.R., Investigation of gas flow in micro-filters and modification of scaling law. International Communications in Heat and Mass Transfer, 36 (7), 763–767, (2009).

[104] Karniadakis G. E., Beskok A. and Aluru N., Microflows: Fundamentals and Simulation, Springer, New York (2005).

[105] Kennard E. H., Kinetic Theory of Gases with an Introduction to Statistical Mechanics, Allied Pacific, Bombay, (1962).

[106] Khadem M. H., Shams M. and Hossainpour S., Numerical simulation of roughness effects on flow and heat transfer in microchannels at slip flow regime, International Communications in Heat and Mass Transfer, 36, 69–77, (2009).

[107] Knechtel, E.D. and Pitts, W.C., Normal and tangential momentum accommodation for earth satellite conditions, Astronautica Acta, 18, 171–184 (1973).

[108] Knudsen M., Kinetic Theory of Gases. John Wiley, New York, (1950).

[109] Kohl M.J, Abdel-Khalik S.I., Jeter S.M., Sadowski D.L., An experimental investigation of microchannel flow with internal pressure measurements, Int. J. Heat and Mass Transfer, 48, 1518–1533, (2005).

[110] Kuhlthau A.R., Air friction on rapidly moving surfaces, Journal of Applied Physics, 20, 217–223 (1949).

[111] Kuscar I, Phenomenology of gas-surface accommodation. Rarefied Gas Dynamics, Proceedings of the Ninth International Symposium, edited by M. Becker and M. Fiebig DFVLR, Porz-Wahn, Germany, Paper No. E. 1–1, (1974).

[112] Lee S.Y.K., Wong M. and Zohar Y., Gas flow in microchannels with bend, J. Micromech. Microeng., 11, 635–644, (2001).

[113] Lee T. and Lin C.L., Rarefaction and compressibility effects of the lattice-Boltzmann-equation method in a gas microchannel, Physical Review E, 71, 046706, (2005).

[114] Lee W.Y., Wong M. and Zohar Y., Microchannels in series connected via a contraction/expansion section, J. Fluid Mech., 459, 187–206, (2002).

[115] Lewandowski T., Jebauer S., Czerwinska J., Doerffer P., Entrance Effects in Microchannel Gas Flow. Journal of Thermal Science, 18 (4), 345–352, (2009).

[116] Li B. and Kwok D. Y., Discrete Boltzmann Equation for Microfluidics, Physical Review Letters, 90, 124502, (2003).

[117] Li C, Li J. and Zhang T., The Entrance Effect on Gases Flow Characteristics in Micro-tube. Journal of Thermal Science, 18 (4), 353–357, (2009).

[118] Li Q., He Y. L., Tang G. H. and Tao W. Q., Lattice Boltzmann modeling of microchannel flows in the transition flow regime. Microfluid Nanofluid, 10, 607–618, (2011).

[119] Lim C. Y., Shu C., Niu X. D. and Chew Y. T., Application of lattice Boltzmann method to simulate microchannel flows, Physics of Fluids, 14 (7), 2299–2308, (2002).

[120] Liu C.F. and Ni Y.S., The fractal roughness effect of micro Poiseuille flows using the lattice Boltzmann method, International Journal of Engineering Science, 47 (5–6), 660–668, (2009).

[121] Liu J, Tai Y C and Ho C M, MEMS for pressure distribution studies of gases flows in microchannels, IEEE MEMS, 209, (1995).

[122] Liu X. and Guo Z., A lattice Boltzmann study of gas flows in a long micro-channel, Computers and Mathematics with Applications, 2011, to appear

[123] Lockerby D.A. and Reese J.M., On the modeling of isothermal gas flows at the microscale. Journal of Fluid Mechanics, 604, 235–261, (2008).

[124] Lockerby D.A., Reese J.M., Emerson D.R. and Barber R.W. Velocity boundary condition at solid walls in rarefied gas calculations. Physical Review E, 70, 017303, (2004).

[125] Lord R. G., Tangential Momentum Accommodation Coefficients of rare Gases on Polycrystalline Metal Surfaces. 10th International Symposium, Aspen, Colorado, 18–23 July 1976, 531–538 (1977).

[126] Lorenzini M., Morini G.L. and Salvigni S., Laminar, transitional and turbulent friction factors for gas flows in smooth and rough microtubes, International Journal of Thermal Sciences, 49, 248–255, (2010).

[127] Khan M. G. and Fartaj A., A review on microchannel heat exchangers and potential applications, Int. J. Energy Res., 35, 553–582, (2011).

[128] Maharudrayya S., Jayanti S. and Deshpande A. P., Pressure losses in laminar flow through serpentine channels in fuel cell stacks, Journal of Power Sources, 138, 1–13, (2004).

[129] Mahulikar S.P., Herwig H., and Hausner O., Study of Gas Microconvection for Synthesis of Rarefaction and No rarefaction Effects, Journal of Microelectromechanical systems, 16 (6), 1543–1556, (2007).

[130] Marino L., Experiments on rarefied gas flows through tubes. Microfluidics and Nanofluidics, 6, 109–119, (2009).

[131] Maurer J., Tabeling P., Joseph P. and Willaime H., Second-order slip laws in micro-channels for helium and nitrogen, Physics of Fluids, 15 (9), 2613–2621, (2003).

[132] Mavriplis C., Ahn J. C. and Goulard R., Heat Transfer and Flowfields in Short Microchannels Using Direct Simulation Monte Carlo, Journal of Thermophysics and Heat Transfer, 11 (4), 489–496, (1997).

[133] Michalis V.K., Kalarakis A.N., Skouras E.D. and Burganos V.N., Rarefaction effects on gas viscosity in the Knudsen transition regime. Microfluidics and Nanofluidics 9(4–5), 847–853, (2010).

[134] Millikan R.A., Coefficients of slip in gases and the law of reflection of molecules from the surfaces of solids and liquids, Physical Review, 21, 217–238 (1923).

[135] Mo G. and Rosenberger F., Molecular-dynamics simulation of flow in a two-dimensional channel with atomically rough walls, Physical Review A, 42 (8), 4688–4692, (1990)

[136] Morini G.L., Lorenzini M. and Salvigni S., Friction characteristics of compressible gas flows in microtubes. Experimental Thermal and Fluid Science, 30, 733–744, (2006).

[137] Morini G.L., Lorenzini M., Colin S. and Geoffroy S., Experimental analysis of pressure drop and laminar to turbulent transition for gas flows in smooth microtubes. Heat Transfer Engineering, 28, 670–679, (2007).

[138] Morini G.L., Single-phase convective heat transfer in microchannels: a review of experimental results, International Journal of Thermal Sciences 43, 631–651, (2004).

[139] Morini G.L., Spiga M. and Tartarini P., Rarefaction effects on friction factor of gas flow in microchannels. Super lattices and Microstructures, 35, 587–599, (2004).

[140] Morini G.L., Yang Y., Chalabi H. and Lorenzini M., A critical review of the measurement techniques for the analysis of gas microflows through microchannels. Experimental Thermal and Fluid Science, 35, 849–865, (2011).

[141] Mott D.R., Oran E.S. and Kaplan C.R., Microfilter simulations and scaling law AIAA J. Thermophys. Heat Transfer, 15, 473–477, (2001).

[142] Naris S. and Dimitris V., Rarefied gas flow in a triangular duct based on a boundary fitted lattice. European Journal of Mechanics B, 27, 810–222, (2007).

[143] Nedea S.V., Frijns A.J.H., van Steenhoven A.A., Markvoort A.J. and Hilbers P.A.J., Hybrid method coupling molecular dynamics and Monte Carlo simulations to study the properties of gases in microchannels and nanochannels, Physical Review E, 72, 016705, (2005).

[144] Nie X, Doolen G. D. and Chen S., Lattice Boltzmann Simulation of Fluid Flow in MEMS, Journal of Statistical Physics, 107, 279–289, (2002).

[145] Niu X.D., Shu C. and Chew Y.T., A lattice Boltzmann BGK model for simulation of micro flows, Europhys. Lett., 67 (4), 600–606, (2004).

[146] Niu X.D., Shu C. and Chew Y.T., Numerical simulation of isothermal micro flows by lattice boltzmann method and theoretical analysis of the diffuse scattering boundary condition, Int. J. of Modern Physics C, 16 (12), 1927–1941, (2005).

[147] Oh C.K., Oran E.S. and Sinkovits R.S., Computations of high-speed, high Knudsen number microchannel flows, Journal of Thermophysics and Heat Transfer, 11 (4), 497–505, (1997).

[148] Palle S. and Aliabadi S., Slip flow and heat transfer in rectangular and circular microchannels using hybrid FE/FV method. Int. J. Numer. Meth. Engng (2011), to appear.

[149] Pan L.S., Liu G.R. and Lam K.Y., Determination of slip coefficient for rarefied gas flows using direct simulation Monte Carlo, Journal of Micromechanics and Microengineering, 9, 89 (1999).

[150] Pfahler J., Harley J.C., Bau H. and Zemel J.N., Gas and liquid flow in small channels ASME, DSC-32 49–60, (1991).

[151] Piekos E.S. and Breuer K.S., Numerical Modeling of Micromechanical Devices Using the Direct Simulation Monte Carlo Method, J. Fluids Eng., 118 (3), 464–469, (1996).

[152] Pitakarnnop J., Varoutis S., Valougeorgis D., Geoffroy, S. Baldas L. and Colin S., A novel experimental setup for gas microflows. Microfluidics and Nanofluidics, 8, pp. 57–72, (2010).

[153] Pong K., Ho C. M., Liu J. and Tai Y.C., Non-linear pressure distribution in uniform microchannels, Proc. of Appl. Microfabrication to Fluid Mech., ASME Winter Annual Meeting, Chicago, pp. 51–56, (1994).

[154] Porodnov B.T., Suetin P.E., Borisov S.F. and Akinshin V.D., Experimental investigation of rarefied gas flow in different channels, Journal of Fluid Mechanics, 64, 417–438 (1974).

[155] Raghavan V. and Premachandran B., Microscale flow through channels with a right angled bend: effect of fillet radius, J. Fluids Engineering, 130, 101207, (2008).

[156] Raju C., Kurian J., Experimental investigation of rarefied gas flow through rectangular slits and nozzles, Experiment in Fluids 17, 220-224, (1994).

[157] Raisee M. and Vahedi N., Prediction of Gas Flow Through Short and Long 2-D Micro- and Nanochannels Using a Generalized Slip Model, Heat Transfer Engineering, 31 (8), 675–681, (2010).

[158] Raju R. and Roy S., Hydrodynamic model for microscale flows in a channel with two 90° bends, Proceedings of FEDSM'03, 4th ASME/JSME Joint Fluids Engineering Conference, Paper no. FEDSM2003-45535, (2003).

[159] Rashidi M.M., Ganji D.D. and Shahmohamadi H., Variational iteration method for two-dimensional steady slip flow in micro-channels, Archive of Applied Mechanics, DOI: 10.1007/s00419-010-0504-x, 2011, to appear

[160] Rathakrishnan E. and Sreekanth A.K., Rarefied flow through sudden enlargements, Fluid Dynamics Research, 16, 131–145, (1995).

[161] Reese J.M., Gallis M.A. and Lockerby D.A., New directions in fluid dynamics: non-equilibrium aerodynamic and microsystem flows. Phil. Trans. R. Soc. Lond. A, 361, 2967–2988, (2003).

[162] Renksizbulut M., Niazmand H. and Tercan G., Slip-flow and heat transfer in rectangular microchannels with constant wall temperature. International Journal of Thermal Sciences 45, 870–881, (2006).

[163] Richardson S., On the no-slip boundary condition, J. Fluid Mech, 59 (4), 707–719, (1973).

[164] Ritos K., Lihnaropoulos Y., Naris S. and Valougeorgis D., Pressure- and Temperature-Driven Flow Through Triangular and Trapezoidal Microchannels. Heat Transfer Engineering, 32 (13–14), 1101–1107, (2011).

[165] Rostami A.A., Mujumdar A.S. and Saniei N., Flow and heat transfer for gas flowing in microchannels: a review, Heat and Mass Transfer 38, 359–367, (2002).

[166] Roy S. and Chakraborty S., Near-wall effects in micro scale Couette flow and heat transfer in the Maxwell-slip regimes. Microfluid Nanofluid, 3, 437–449, (2007).

[167] Roy S., Raju R., Chuang H.F., Cruden B.A. and Meyyappan M., Modeling gas flow through microchannels and nonporous, Journal of Applied Physics, 93 (8), 4870–4879, (2003).

[168] Saha M.N. and Srivastava B.N., A Treatise on Heat. Indian Press, Allahabad, (1958).

[169] Saxena I., Agrawal A. and Joshi S.S., Fabrication of microfilters using excimer laser micromachining and testing of pressure drop. J. Micromech. Microeng. 19, 025025, (2009).

[170] Schaaf S.A. and Chambre P.L., Flow of Rarefied Gases. Princeton University Press (1961).

[171] Shah R.K. and London A.L., Laminar Flow Forced Convection in Ducts, Advances in Heat Transfer Series, New York: Academic (1978).

[172] Shams M., Shojaeian M., Aghanajafi C. and Dibaji S.A.R., Numerical simulation of slip flow through rhombus microchannels. International Communications in Heat and Mass Transfer 36, 1075–1081, (2009).

[173] Sharipov F. and Seleznev V., Data on internal rarefied gas flows, J. Phys. Chem. Ref. Data, 27, 657–706, (1998).

[174] Shen C, Fan J. and Xie C., Statistical simulation of rarefied gas flows in micro-channels, Journal of Computational Physics, 189, 512–526, (2003).

[175] Shen C, Tian D. B., Xie C. and Fan J., Examination of the LBM in simulation of microchannel flow in transitional regime, Microscale Thermophysical Engineering, 8, 423–432, (2004).

[176] Shen C, Use of the degenerated Reynolds equation in solving the microchannel flow problem, Physics of Fluids, 17, 046101, (2005).

[177] Shields F.D., Energy and momentum accommodation coefficients on platinum and silver, Journal of Chemical Physics, 78, 3329–3333 (1983).

[178] Shields F.D., More on the acoustical method of measuring energy and tangential momentum accommodation coefficients, Journal of Chemical Physics, 72, 3767–3772 (1980).

[179] Shih J.C., Ho C.M., Liu J. and Tai Y.C., Monatomic and polyatomic gas flow through uniform microchannels, ASME, DSC-59 197, (1996).

[180] Shinagawa H., Setyawan H., Asai T., Sugiyama Y. and Okuyama K., An experimental and theoretical investigation of rarefied gas flow through circular tube of finite length. Chemical Engineering Science, 57, 4027–4036, (2002).

[181] Shirani E. and Jafari S., Application of LBM in Simulation of Flow in Simple Micro-Geometries and Micro Porous Media, African Physical Review, 1, 34–42, (2007).

[182] Shojaeian M. and Dibaji S.A.R., Three-dimensional numerical simulation of the slip flow through triangular microchannels. International Communications in Heat and Mass Transfer 37, 324–329, (2010).

[183] Shokouhmand H., Bigham S. and Isfahani R.N., Effects of Knudsen number and geometry on gaseous flow and heat transfer in a constricted microchannel. Heat Mass Transfer, 47, 119–130, (2011).

[184] Shu C., Niu X.D., and Chew Y.T., A Lattice Boltzmann Kinetic Model for Microflow and Heat Transfer, Journal of Statistical Physics, 121, 239–255 (2005).

[185] Sidik N.A.C., Horng N.C., Mussa M.A. and Abdullah S., Simulation of Rarefied Gas Flow in Slip and Transitional Regimes by the Lattice Boltzmann Method, CFD Letters, 2(2), 66–74, (2010).

[186] Sobhan C.B. and Garimella S.V., A comparative analysis of studies on heat transfer and fluid flow in microchannels, Microscale Thermophysical Engineering 5, 293–311, (2001).

[187] Sofonea V. and Sekerka R.F., Boundary conditions for the upwind finite difference Lattice Boltzmann model: Evidence of slip velocity in micro-channel flow, Journal of Computational Physics, 207, 639–659, (2005).

[188] Sreekanth A.K., Slip flow through long circular pipes, L. Trilling, H.Y. Wachman, Editors, Proceedings of the Sixth International Symposium on Rarefied Gas Dynamics, Academic Press, 667–680, (1969).

[189] Stacy L.J., A determination by the constant deflection method of the value of the coefficient of slip for rough and for smooth surfaces in air, Physical Review 21, 239–249 (1923).

[190] Stevanovic N D, A new analytical solution of microchannel gas flow. J. Micromech. Microeng. 17, 1695–1702, (2007).

[191] Stops D.W., The mean free path of gas molecules in the transition regime, J. Phys. D, 3, 685, (1970).

[192] Succi S., The Lattice Boltzmann Equation: For Fluid Dynamic and Beyond Series Numerical Mathematics and Scientific Computation, Oxford University Press, (2001).

[193] Succi S., Mesoscopic modeling of slip motion at fluid-solid interfaces with heterogenous catalysis, Phys. Rev. Lett. 89, 064502, (2002).

[194] Suetin P.E., Porodnov B.T., Chernjak V.G. and Borisov S.F., Poiseuille flow at arbitrary Knudsen numbers and tangential momentum accommodation, Journal of Fluid Mechanics, 60, 581–592 (1973).

[195] Sugiyama W., Sawadaa T. and Kenji N., Rarefied gas flow between two flat plates with two dimensional surface roughness, Vacuum, 47, 791–794 (1996).

[196] Sun H. and Faghri M., Effects of rarefaction and compressibility of gaseous flow in microchannel using DSMC, Numerical Heat Transfer A, 38, 153–168, (2000).

[197] Sun H.W. and Faghri M., Effect of surface roughness on nitrogen flow in a microchannel using the direct simulation Monte Carlo method, Num. Heat Transfer Part A, 43, 1, (2003).

[198] Sun Q. and Boyd I.D., A Direct Simulation Method for Subsonic Microscale Gas Flows, Journal of Computational Physics, 179, 400–425, (2002).

[199] Szalmas L. and Valougeorgis D., Rarefied gas flow of binary mixtures through long channels with triangular and trapezoidal cross sections. Microfluidics and Nanofluidics, 9, 471–487, (2010).

[200] Taheri P. and Struchtrup H., An extended macroscopic transport model for rarefied gas flows in long capillaries with circular cross section. Physics of Fluid 22, 112004, (2010).

[201] Tang G.H., Li Z., He Y.L. and Tao W.Q., Experimental study of compressibility, roughness and rarefaction influences on microchannel flow, International Journal of Heat and Mass Transfer, 50, 2282–2295, (2007).

[202] Tang G.H., Tao W.Q. and He Y.L., Lattice Boltzmann method for gaseous microflows using kinetic theory boundary conditions, Phys. Fluids, 17, 058101, (2005).

[203] Tekasakul P., Bentz J.A., Tompson R.V. and Loyalka S.K., The spinning rotor gauge: Measurements of viscosity, velocity slip coefficients, and tangential momentum accommodation coefficients, Journal of Vacuum Science and Technology A, 14, 2946–2952 (1996).

[204] Tian Z.W., Zou C., Liu H.J., Guo Z.L., Liu Z.H. and Zheng C.G., Lattice Boltzmann scheme for simulating thermal micro-flow, Physica A, 385, 59–68, (2007).

[205] Timiriazeff, A. ber die innere Reibung verdnnter Gase und ber den Zusammenhang der Gleitung und des Temperatursprunges an der Grenze zwischen Metall und Gas, Annalen der Physik, 345, 971–991 (1913) (in German).

[206] Tison S.A., Experimental Data and Theoretical Modeling of Gas Flows through Metal Capillary Leaks, Vacuum 44, 1171–1175, (1993).

[207] Toschi F. and Succi S., Lattice Boltzmann method at finite Knudsen numbers. Europhysics Letters 69 (4), 549–555, (2005).

[208] Tuckerman D.B. and Pease R.F.W., High-performance heat sinking for VLSI. IEEE Electron Device Letters, 2 (5), 126–129, (1981).

[209] Turner S.E., Lam L.C., Faghri M. and Gregory O.J., Experimental Investigation of Gas Flow in Microchannels, Journal of Heat Transfer, 126, 753–763, (2004).

[210] Valougeorgis, D. The friction factor of a rarefied gas flow in a circular tube. Physics of Fluids, 19, 091702, 2007.

[211] van Dyke K.S., The coefficients of viscosity and of slip of air and of carbon dioxide by the rotating cylinder method, Physical Review 21, 250–265 (1923).

[212] Varade V., Pradeep A, Prabhu S. and Agrawal A., Experimental study of rarefied gas flow through a 90° bend tube, 2nd European Conference on Microfluidics – 2010, Toulouse, France, December 2010.

[213] Varoutis S., Valougeorgis D. and Sharipov F., Simulation of gas flow through tubes of finite length over the whole range of rarefaction for various pressure drop ratios, J. Vac. Sci. Technol. A, 27, 1377–1391, (2009a).

[214] Varoutis S., Naris S., Hauer V., Day C. and Valougeorgis D., Computational and experimental study of gas flows through long channels of various cross sections in the whole range of the Knudsen number. J. Vac. Sci. Technol. A 27(1), 89–100, (2009b).

[215] Verhaeghe F., Luo L.S. and Blanpain B., Lattice Boltzmann modeling of microchannel flow in slip flow regime, Journal of Computational Physics, 228, 147–157, (2009).

[216] Verma B., Demsis A., Agrawal A. and Prabhu S.V., Semi-empirical correlation for friction factor with gas flow through smooth microtube. Journal of Vacuum Science and Technology A, 27, 584–590, (2009).

[217] Vijayalakshmi K., Anoop K.B., Patel H. E., Harikrishna P.V., Sundararajan T. and Das S.K., Effects of compressibility and transition to turbulence on flow through microchannels, International Journal of Heat and Mass Transfer, 52, 2196–2204, (2009).

[218] Vimmr J., Klášterka H., Hajžman M., Luxa M. and Dvořák R., Mathematical Modelling and Experimental Investigation of Gas Flow in Minichannels and Microchannels. Journal of Thermal Science, 19 (4), 289–294, (2010).

[219] Volkov I.V., Gas-dynamic boundary conditions of slip on an uneven surface, U.S.S.R. Comput. Maths. Math. Phys., 28 (l), 52–58, (1988).

[220] Wang M. and Li Z., Micro- and nanoscale non-ideal gas Poiseuille flows in a consistent Boltzmann algorithm model, J. Micromech. Microeng., 14, 1057–1063, (2004).

[221] Wang M. and Li Z., Nonideal gas flow and heat transfer in micro- and nanochannels using the direct simulation Monte Carlo method, Physical Review E, 68, 046704, (2003).

[222] Wang M. and Li Z., Simulations for gas flows in microgeometries using the direct simulation Monte Carlo method, Int. J. Heat and Fluid Flow, 25, 975–985, (2004a).

[223] Wang M.R. and Li Z.X., Numerical simulations on performance of MEMS-based nozzles at moderate or low temperatures, Microfluidics and Nanofluidics, 1, 62–70, (2004b).

[224] Wu J.S., Lee F and Wong S.C., Pressure boundary treatment in micromechanical devices using the direct simulation Monte Carlo method, JSME International Journal B, 44 (3), 439–450, (2001).

[225] Wu P.Y. and Little W.A., Measurement of friction factors for the flow of gases in very fine channels used for microminiature Joule–Thomson refrigerators, Cryogenics, 23, 273–277, (1983).

[226] Wuest W., Boundary layers in rarefied gas flow, Progress in Aerospace Science, 8, 295–352 (1967).

[227] Xu K. and Li Z. Microchannel flow in the slip regime: gas-kinetic BGK–Burnett solutions, J. Fluid Mech., 513, 87–110, (2004).

[228] Xu K., Super-Burnett solutions for Poiseuille flow. Phys. Fluids 15 (7), 2077–2080, (2003).

[229] Xue H., Fan Q. and Shu C., Prediction of micro-channel flows using direct simulation Monte Carlo, Probabilistic Engineering Mechanics, 15, 213–219, (2000).

[230] Xue H., Ji H.M. and Shu C., Analysis of micro-Couette flow using the Burnett equations. Int. J. Heat and Mass Transfer, 44, 4139–4146, (2001).

[231] Yamaguchi H., Hanawa T., Yamamoto O., Matsuda Y., Egami Y., Niimi T., Experimental measurement on tangential momentum accommodation coefficient in a single microtube. Microfluid Nanofluid, 11, 57–64, (2011).

[232] Yamamoto K., Slip flow over a smooth platinum surface, JSME International Journal B, 45, 788–795 (2002).

[233] Yan F. and Farouk B., Computations of Low Pressure Fluid Flow and Heat Transfer in Ducts Using the Direct Simulation Monte Carlo Method, J. Heat Transfer, 124 (4), 609–616, (2002).

[234] Yan X., Wang Q. and Suo X., Investigation of Flow Resistance in Microchannels with a Sudden Contraction or Expansion Using DSMC, ASME, First International Conference on Micro/Nanoscale Heat Transfer, Parts A and B, MNHT, 52172, 715–721, (2008).

[235] Yang J M, Yang X, Ho C M and Tai Y C, Micromachined particle filter with low power dissipation, J. Fluids Eng., 123, 899–908, (2001).

[236] Yang J., Ye J. J., Zheng J. Y., Wong I., Lam C. K., P. Xu P., Chen R. X. and Zhu Z. H., Using Direct Simulation Monte Carlo With Improved Boundary Conditions for Heat and Mass Transfer in Microchannels. Journal of Heat Transfer, 132, 041008, 2010.

[237] Yang X., Yang J.M., Tai Y.C. and Ho C.M., Micromachined membrane particle filters, Sensors Actuators, 73, 184–91, 1999.

[238] Yoon S., Ross J., Mench M. and Sharp K., Gas-phase particle image velocimetry (PIV) for application to the design of fuel cell reactant flow channels. Journal of Power Sources, 160, 1017–1025, (2006).

[239] Zahid W.A., Yin Y. and Zhu K.Q., Couette–Poiseuille flow of a gas in long microchannels, Microfluid Nanofluid, 3, 55–64, (2007).

[240] Zahmatkesh I., Alishahi M.M. and Emdad H., New velocity-slip and temperature-jump boundary conditions for Navier–Stokes computation of gas mixture flows in microgeometries, Mechanics Research Communications 38, 417–424, (2011).

[241] Zhang T., Jia Li and Wang Z., Validation of Navier–Stokes equations for slip flow analysis within transition region, International Journal of Heat and Mass Transfer, 51, 6323–6327, (2008).

[242] Zhang T.T., Jia L., Wang Z.C. and Li C.W., Slip flow characteristics of compressible gaseous in microchannels, Energy Conversion and Management, 50, 1676–1681, (2009).

[243] Zhang T.T. and Jia Li, Numerical Simulation of Roughness Effect on Gaseous Flow and Heat Transfer in Microchannels, Proceedings of the 2nd IEEE International Conference on Nano/Micro Engineered and Molecular Systems, January 16 - 19, 2007, Bangkok, Thailand, (2007).

[244] Zhang Y. H., Qin R. S., Sun Y. H., Barber R.W. and Emerson D.R., Gas Flow in Microchannels – A Lattice Boltzmann Method Approach, Journal of Statistical Physics, 121, 257–267, (2005a).

[245] Zhang Y., Qin R., and Emerson D. R., Lattice Boltzmann simulation of rarefied gas flows in microchannels, Phys. Rev. E 71, 047702, (2005b).

[246] Zhao H., The numerical solution of gaseous slip flows in microtubes. Int. Comm. Heat Mass Transfer, 28 (4), 585–594, (2001).

[247] Zhou Y., Zhang R., Staroselsky I., Chen H., Kim W.T. and Jhon M.S., Simulation of micro- and nano-scale flows via the lattice Boltzmann method, Physica A: Statistical Mechanics and its Applications, 362 (1), 68–77, (2006).

[248] Ziarani A. S. and Mohamad A. A., Effect of wall roughness on the slip of fluid in a microchannel, Nanoscale and Microscale Thermophysical Engineering, 12, 154–169, (2008).

[249] Zohar Y., Lee S.Y.K., Lee W.Y., Jiang L. and Tong P., Subsonic gas flow in a straight and uniform microchannel, J. Fluid Mech. 472, 125–151, (2002).